University of Siena

Doctorate in Biomedicine and Immunological Sciences

Section of Clinical Pharmacology

XXV Cycle

Comparative analysis of P2X7 receptor expression in EAE rat model and MS tissue

Tutor

Prof. Franco Laghi Pasini

PhD Student

Cinzia Montilli

Academic Year 2012/2013

Contents

Abbreviations

AD	Alzheiner’s disease
ADP	adenosine diphosphate
ALS	amyotrophic lateral sclerosis
ATP	adenosine triphosphate
BBB	blood brain barrier
BzATP	2'(3')-O-(4-benzoylbenzoyl)adenosine-5'-triphosphate
CFA	complete Freund’s adjuvant
CNS	central nervous system
dpi	days post- injection
EAE	experimental autoimmune encephalomyelitis
EBV	Epstein-Barr virus
FST	forced-swim test
GFAP	glial fibrillary acidic protein
GM	grey matter
HD	Huntington’s disease
HLA	human leukocyte antigen
IL-1β	interleukin-1β
IL7Rα	interleukin 7 receptor α subunit
LPS	lipopolysaccharide
MBP	myelin basic protein
MHCII	major histocompatibility complex II
MOG	myelin oligodendrocyte glycoprotein
MS	multiple sclerosis
MW	molecular weight
NDS	normal donkey serum
OPCs	oligodendrocyte progenitor cells
P2X7R	P2X7 receptor
Panx1	pannexin-1
PBMCs	peripheral blood mononuclear cells
PBS	phosphate buffer saline
PD	Parkinson’s disease
PPMS	primary progressive multiple sclerosis
RRMS	relapsing/remitting multiple sclerosis
SPMS	secondary progressive multiple sclerosis
WM	white matter

Introduction

1.1 Purinergic classification

Purinergic receptors were first defined in 1976 by G. Burnstock and 2 years later a basis for distinguishing two types of purinoceptor, identified as P1 and P2 (for adenosine and ATP/ADP, respectively), was proposed. For P1 receptors, four subtypes termed A1, A2A, A2B, and A3A were identified [1], while two types of P2 receptor were recognized and respectively P2X family of ligand-gated ion channels (named ionotropic receptors) responsible for fast excitatory neurotransmission, and P2Y family of G protein-coupled receptors (named metabotropic receptors) possessing slow excitatory responses [2] (Fig. 1). This nomenclature has been widely adopted, and currently seven P2X subunits (P2X 1-7) and eight P2Y receptor subtypes (P2Y 1,2,4,6,11-14) are documented and shown to be activated by extracellular ATP and its analogues [3].

Considering its importance in cell signalling, the concentration of extracellular nucleotides is tightly regulated by a variety of cell surface-located enzymes named ectonucleotidases. These enzymes are capable of hydrolysing nucleoside triphosphates, diphosphates and monophosphates to their respective nucleosides [4]. There are four major families of ectonucleotidases, ectonucleoside triphosphate diphosphohydrolases, ectonucleotide pyrophosphate/phosphodiesterases, alkaline phosphatases and ecto-5'-nucleotidase [5]. In several tissues and cells, ectonucleotidases operate jointly with other enzymes such as adenylate kinase, nucleoside diphosphate kinase, ecto-F1–Fo ATP synthases, and CD38/NADase to form a complex cell surface-localized machine for nucleotide hydrolysis. In addition to their role in the inactivation of purinergic signalling, ectonucleotidases have been proposed to prevent P2 receptor desensitization and control the availability of ligands to nucleotide and adenosine receptors [6].

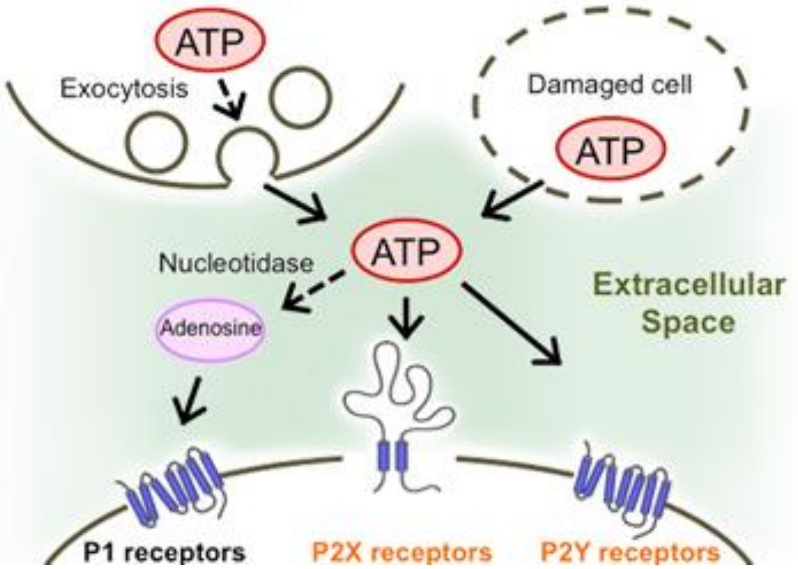

Fig 1. From: The Kawate Laboratory Department of Molecular Medicine, Cornell University

1.2 The P2X7 receptor (P2X7R)

a) Genetics

In 1997, Rassendren et al. [7] cloned the human gene for a receptor, called *P2RX7* that was structurally related to the P2X family. They screened a human monocyte cDNA library with the rat *P2RX7* gene as a probe, and recovered a cDNA encoding a predicted 595-amino acid protein that was 80% identical to the rat P2X7R protein. *P2RX7* is expressed as a 6-kb mRNA in many tissue.

The *P2RX7* gene contains 13 exons and is localized close to the tip of the long arm of human chromosome 12(q24.31) [8]. Alternative splicing, which enables one gene to produce multiple protein isoforms, is responsible for 23 P2RX7 mRNA transcripts listed in the NCBI database, of which 18 are predicted to encode P2X7 protein variants. These include the full-length variant, P2X7(a), and two human isoforms, P2X7(b) [9] and P2X7(j) [10]. Only the P2X7(b) isoform has been fully characterized in functional studies, and while P2X7(b) has ATP-stimulated channel activity when transfected into HEK-293 cells, it is unable to form a homotrimeric pore. Furthermore, P2X7(b) has been shown to co-assemble with full-length P2X7 into a heterotrimer

that potentiated P2X7 responses to ATP, including channel and pore formation and membrane blebbing.

b) Protein structure

In 1997, Hansen *et al*. [11] studied the topology of P2X7R on the plasma membrane, establishing that amino acids N-1-25 reside on the cytoplasmic side, amino acids 26-46 constitute the highly hydrophobic transmembrane TM1 region, amino acids 47-334 are responsible for the extracellular loop (containing the ATP binding site), amino acids 335-355 form the transmembrane TM2 region and amino acids 356-595-C are present on the cytoplasmic side. The N terminus has residues related to selectivity and activity of the ion channel and interaction with mitogen-activated protein kinases [12]. Only one α-helix is predicted in the TM1 segment, and a major propensity for β-sheet conformation is expected in the TM2 region [13]. Some residues of the extracellular loop displaying three different binding sites for ATP are glycosylated in the ATP-interacting sequence. The intracellular COOH terminus (239 amino acids) is much longer than in all other P2XR subtypes, and is involved in the majority of functions related to P2X7R and contains an additional hydrophobic domain (residues 510-530) sufficiently long to traverse the plasma membrane [14].

Substantial evidence supports a trimeric structure for P2X7R, although scattered evidence suggests that it might aggregate to form hexamers [15]. It has been suggested that it forms heteromers with P2X4R [16]. However, in another study using subtype-specific antibodies in combination with blue native polyacrylamide gel electrophoresis (to directly visualize P2X receptor complexes solubilized from membrane extracts of a wide variety of tissues), homotrimeric complexes were the dominant assembly state of P2X7R complexes. No complexes corresponding to more than three subunits or heterotrimeric P2X4R/P2X7R were detected, suggesting that either higher heteromerization between P2X4R and P2X7R subunits results in unstable heteromeric complexes, or that such P2X4R/P2X7R heteromers do not represent a dominant subtype in the tissues investigated [17]. However, a variety of proteins interacting with the P2X7R have been identified by immunoprecipitation of P2X7R overexpressed in HEK cells [18] and, moreover, in a yeast two-

hybrid screen [19]. Transient interaction *via* one of these proteins could also account for these copurification results [20,21].

c) Permeability and currents

In contrast to other P2X receptors, stimulation of the P2X7R subtype with high concentrations of ATP is associated with two different membrane permeability states: a small nonselective monovalent and divalent cation conductance (Ca2+ and Na+ influx and K+ efflux), which opens within milliseconds after brief agonist stimulation, leading to depolarization of the plasma membrane [22], followed by increased non-selective membrane permeability to larger cations such as N-methyl-D-glucamine (MW, molecular weight 195) after prolonged and repetitive agonist stimulation [23]. Membrane permeability increases with time, allowing cellular uptake of higher MW fluorescent dyes such as ethidium bromide (MW 394) or Yo-Pro-1 (MW 629). This phenomenon has been attributed to the formation of large cytolytic pores in the plasma membrane, often leading to cell death [24]. This time-dependent increase in permeability has been ascribed to two contrasting mechanisms. The first model allows the coexistence of two functions (channel and large pore) within a single structure [25] and predicts that a conformational change initially forms a channel permeable to small cations, then leading to dilation of the integral P2X7R pore. When ATP at high concentration is bound to P2X7R, eliciting cation influx and intracellular signalling cascades, the β-sheet structure in the TM2 region then assumes a configuration allowing the passage of molecules up to 1 KDa, with the channel transiently acting as a large pore. In addition, P2X7R-mediated pore formation was also reported to result from a coordinated signalling cascade involving both the p38 mitogen-activated protein kinase and caspase pathways that is distinct from other cytolytic pore-forming mechanisms. A selective p38 mitogen-activated protein kinase inhibitor indeed potently inhibits receptor agonist 2'(3')-O-(4-benzoylbenzoyl)adenosine-5'-triphosphate (BzATP)-induced pore formation, without altering P2X7R-mediated calcium influx or interleukin-1β (IL-1β) release. In contrast, caspase inhibitors attenuate both BzATP-induced pore formation and IL-1β release. Taken together, these results support the hypothesis that downstream signalling

mechanisms, rather than channel dilation, mediate cytolytic pore formation after prolonged agonist activation [26]. Moreover, pore opening does not occur in all cell types and may be dependent upon receptor density [22]. P2X7R-mediated changes in calcium influx and pore-opening are species-specific, showing different pharmacological properties between recombinant mouse, rat and human P2X7R [27]. Thus, a constant update of the pharmacology of the P2X7R provides the current advances in the understanding of the biophysical/signalling properties of P2X7R-mediated cation influx and pore formation, and insights into the therapeutic potential of P2X7R antagonists [28].

An alternative mechanism instead postulates the activation of a distinct channel protein permeable to higher MW cations [22]. In this scenario, P2X7R is responsible only for permeability to small cations and interacts instead (directly or through second messengers) with this distinct channel protein, thereby allowing permeability to larger cations. At present, there is no widely accepted hypothesis to explain this phenomenon, and evidence for and against these two models has been forthcoming. The study by Marquesda-Silva *et al*. [29] sheds new light on this confused situation demonstrating that colchicine, independently from disruption of cytoskeletal microtubules, inhibits P2X7R dependent dye uptake without affecting receptor channel ionic currents, thus supporting the hypothesis of a distinct permeation pathway for high MW dyes. However, the molecular nature of this permeation pathway remains unknown. One of the P2X7R activated pore pathways has been attributed to the opening of pannexin-1 (Panx1) hemichannels, allowing the passage of ions and small molecules such as ATP between the intracellular and the extracellular space [30]. This permits further P2X7R activation and induces physiological responses such as spreading of cytoplasmic calcium waves. In particular, the release of ATP through the interaction between Panx1 and P2X7R leads to the release of IL-1β involved in early stages of innate immunity [31]. However, transient P2X7R activation and Ca2+ overload can act as a death trigger for native mouse macrophages independently from Panx1 recruitment [32].

The gating of P2XRs usually consists of three phases: a rapid rising phase of inward current induced by the application of agonist (activation phase), a slowly developing decay phase in the

presence of an agonist (desensitization phase), and a relatively rapid decay of current after ATP is removed (deactivation phase). The main difference among receptors is in their sensitivity for agonists and their activation and desensitization rates [33]. In contrast to other homomeric and heteromeric P2XR, repetitive stimulation with the same agonist concentration causes sensitization of P2X7R, which manifests as a progressive increase in the current amplitude accompanied by a slower deactivation rate. Once a steady level of the secondary current is reached, responses at high agonist concentrations become monophasic. Both phases of response are abolished by the application of AZ10606120, a P2X7R-specific antagonist. These results further support the conclusion that pore dilation accounts for the secondary current growth [34]. Sensitization of the receptors caused by repetitive agonist applications could be partially explained by calcium-CaM signaling [35].

BzATP is the most potent agonist for P2X7R with an EC_{50} value of 50 μM, compared with 3 to 4 mM for ATP. At the sensitized receptor, the EC_{50} values for BzATP and ATP are approximately 25 μM and 2 mM, respectively [27,34].

d) Downstream pathways

After channel opening, the P2X7R is permeable to Na+, K+ and Ca2+. Activation of the P2X7R triggers the efflux of K+ from cells and activates IL-1 converting enzyme, leading to cleavage of pro-IL-1β to mature IL-1β and consequent release from the cell. Many events downstream of P2X7R activation are dependent on extracellular calcium influx. Stimulation of ionotropic P2X7R leads to activation of phospholipases A2 and D (PLA2, D) and protein kinase C (PKC), e.g. resulting in the activation of glycogen synthase kinase 3 (GSK3) or the activation of caspase cascades. Furthermore, the induction of second messenger and enzyme cascades promoted e.g. the activation of mitogen activated protein kinase (MAPK) pathway proteins (ERK1/2), p38 MAPK, and c-Jun N-terminal kinase (JNK), as well as PI3K/Akt. The activity of transcription factors, such as nuclear factor κB (NF-κB), cyclic element-binding protein (CREB), and activator protein (AP-1) are also up-regulated, leading to the expression of proinflammatory genes, such as cyclooxygenase-

2 (COX 2) or inducible nitric oxide synthase (iNOS); this in turn causes the production of arachidonic acid (AA) or nitric oxide (NO), respectively. Finally, the release of ATP via Panx1 hemichannels as well as of ATP and glutamate via P2X7Rs was also found to take place. The present data suggest that P2X7R stimulation is associated with neurological disorders leading to neuroinflammation, and apoptosis. (Fig. 2) [36].

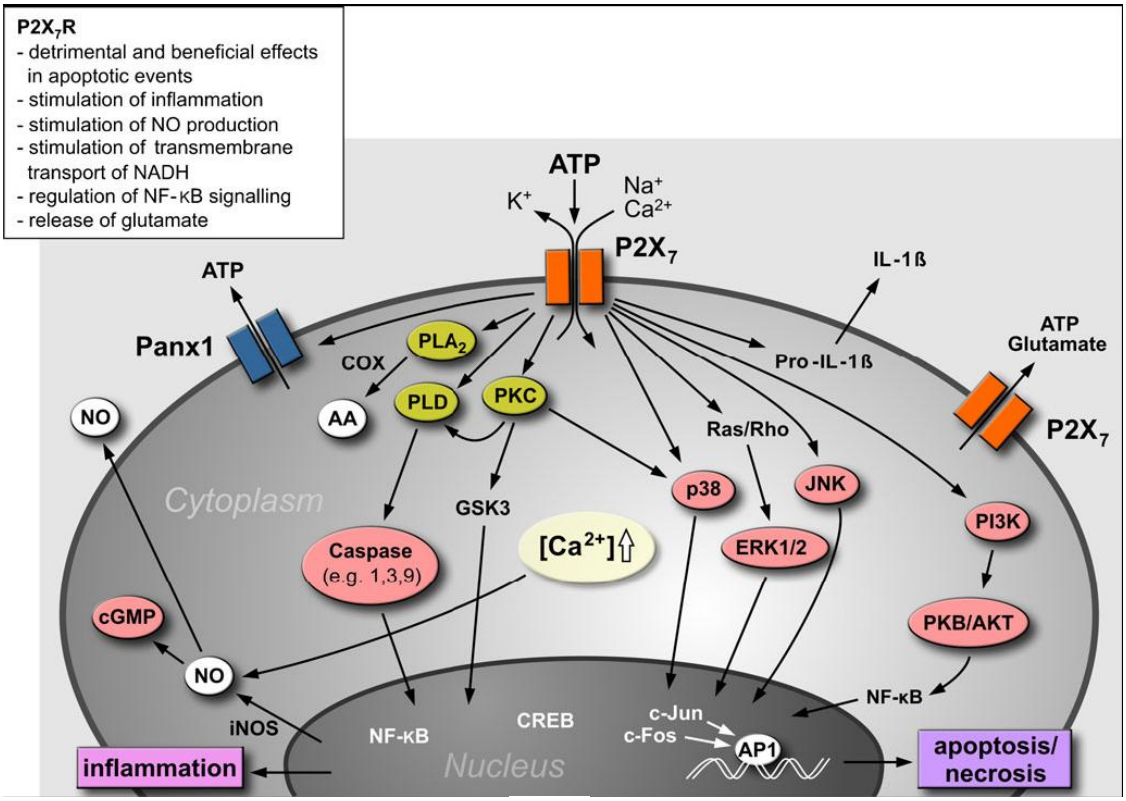

Fig 2. Franke H et al., 2012

e) Tissue distribution and function

P2X7R is selectively expressed on cells of hematopoietic lineage, including mast cells, erythrocytes, monocytes, peripheral macrophages, dendritic cells, T and B lymphocytes, and epidermal Langerhans cells [37]. Many studies have reported that activated microglia express P2X7R at the protein and mRNA levels [38,39], *in vivo* and *in vitro*. Immunohistochemical methods and electrophysiological analyses have shown that P2X7R is also localized on astrocytes [40,41], oligodendrocytes [42] and neurons [43,44], also if these results are still debated in some cases. In situ hybridization showed the expression of P2X7R mRNA also in neurons of hippocampus [45], spinal cord, and medulla oblongata [46], using probes from different regions of

P2X7R cDNA. However, it remains controversial whether P2X7R is actually expressed in astrocytes, neurons, and microglia in the normal rat brain [47]. These discrepancies are due to the fact that the three different currently available P2X7R antibodies show different immunostaining patterns and stain not only brain sections from wild-type mice, but also brain section from P2X7 KO mice. [48]

ATP is the only known physiological activator of the P2X7R [49,50]. Under normal conditions, extracellular ATP is present only in low concentrations. However, the cytoplasmic ATP concentration is in the millimolar range, and activated immune cells [51], macrophages [52], microglia [53], platelets [54], and dying cells [55] may release high concentrations of ATP into the pericellular space. Extracellular ATP concentrations increase significantly under inflammatory conditions *in vivo* [56] and in response to tissue trauma (*e.g.*, ischemia/hypoxia) [57]. The best characterized function of the P2X7R is the IL-1β release from macrophages and microglia activated by substances such as bacterial endotoxin (lipopolysaccharide, LPS) [58].

1.2.1 P2X7R and neuroinflammation/neurodegeneration

Neuroinflammation signifies the brain's patterned response to insult with a number of immunomodulatory responses such as release of cytokines and chemokines set in motion with the activation of microglia. Microglia are resident immune cells of the parenchyma that play important roles in the development of the central nervous system (CNS). At rest or surveilling state, microglia (Fig. 3A) display characteristically ramified morphology with numerous branching processes, used to dynamically monitor the physiological homeostasis of the extracellular space. In response to injury, such as infection or trauma, microglia become activated (Fig 3B), assuming markedly different morphological, biochemical, and immunological states. They retract their ramified processes, develop enlarged somata and numerous lamellipodia, and migrate to the site of injury, proliferate and release proinflammatory cytokines such as IL-1β, IL-6 and TNFα. [59]

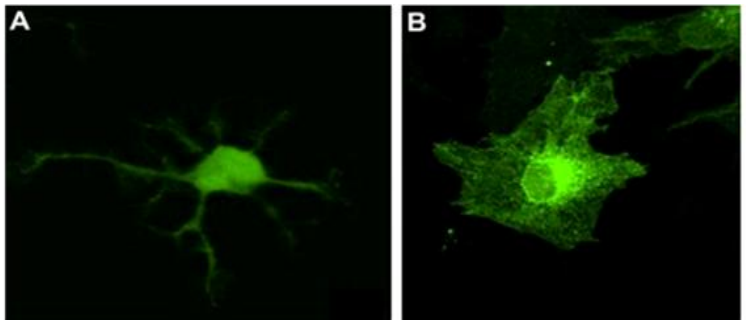

Fig 3. Monif M et al., 2010

Microglial-mediated neuroinflammation is associated with conditions such as Alzheiner's disease (AD), HIV-dementia, Parkinson's disease (PD), prion disease, Amyotrophic Lateral Sclerosis (ALS), and Multiple Sclerosis (MS) [60,61]. Chronic activation of microglia exposes the CNS to various cytokines, chemokines, complement proteins, reactive oxygen species, all of which when present in excessive amounts could have neurotoxic consequences [62]. Activated microglia phagocytose not only damaged cells but also neighbouring healthy cells [63]. For instance during stroke, activated microglia may intensify neuronal death by releasing neurotoxic compounds, as well recruit potentially neurotoxic leukocytes into the injured CNS site [64]. There are numerous reports showing that responses evident in activated microglia, including the release of inflammatory and bio-active substances, can be induced in the same cells by stimulating the P2X7R [65,66].

Interestingly, increased microglial activation and enhanced P2X7R expression are seen in the following conditions: MS and ALS [67], Huntington's disease (HD) [68], prion infection [69], proliferative vitreoretinopathy [70], LPS application to rat striatum [71] , and cerebral ischemia in rodents [38].

In one study increased P2X7R levels and altered receptor-mediated calcium permeability in somata and terminals of neurons from HD mutant mice was observed [68].

Increased expression of P2X7R mRNA has been described in AD-derived microglia compared to non-demented brain, along with prominent P2X7R protein immunoreactivity in association with Aβ plaques and localized to HLA (Human Leucocyte Antigen)-DR-immunoreactive microglia. Intra-hippocampal injection of Aβ in rats resulted in strong P2X7R colocalization with microglia [72] and accumulation of IL-1β in wild-type, but not in P2X7Rdeficient mice [73].

It has also been postulated that abnormal responses to ATP associated with up-regulation of the P2X7R (likely of microglial origin) may participate in the pathophysiology of temporal lobe epilepsy, where activated microglia in the temporal lobe are numerous [74]. Whether P2X7R up-regulation actually led to differentiation was not investigated [66].

Several studies have reported increased P2X7R expression, by immunohistochemistry and Western blot, in the peri-infarct region after middle cerebral artery occlusion in rats [75,39,76].

Le Feuvre *et al*. [77] found that cell death induced by temporary cerebral ischemia was not altered in P2X7R KO mice, but was reduced by treatment with IL-1 receptor antagonist. Treatment of mice with P2X7R antagonists did not affect ischemic or excitotoxic cell death, suggesting that P2X7R is not a primary mediator of experimentally induced neuronal death. In a more recent study, Yanagisawa el al. [76] reported that intracerebroventricular injection with the P2X7R agonist BzATP improved behavioral dysfunction and ischemic neural injury induced by middle cerebral artery occlusion, while the P2X7R antagonist adenosine 5'-triphosphate-2',3'-dialdehyde exacerbated ischemic brain damage.

In ALS patients, as well as in $SOD1^{G93A}$ animals, increased immunoreactivity for P2X7R has been found in spinal cord microglia [78]. Furthermore, $SOD1^{G93A}$ microglia in culture display an increased sensitivity to ATP, and P2X7R activation drives a pro-inflammatory activation that leads to decreased survival of neuronal cell lines [79]. Moreover, P2X7R activation in spinal cord astrocytes has been described to initiate a neurotoxic phenotype that leads to motor neuron death [80].

1.3 Multiple Sclerosis (MS)

a) Epidemiology and Genetics

MS is an inflammatory demyelinating disease of the CNS in which autoreactive myelin-specific T cells cause extensive tissue damage resulting in neurological deficits.

The prevalence of MS has been recorded as >200/100,000 in restricted populations, where artificially high ascertainment inflates estimates [81-82], but is at least 100/100,000 in Canada and higher in the Scandinavian countries (Fig. 4). There is a global latitude gradient with lower prevalence seen nearer the equator [83]. In some isolated communities there is "resistance" to MS, in otherwise high prevalence areas (e.g., the Sámi in Scandinavia) [84]. Generally, MS is of lower prevalence in Asian countries and is more common within populations as socioeconomic status increases [85,86]. There has been a general increase in disease prevalence in the last few decades that cannot be attributed to advances in neuroimaging or changes in diagnostic criteria [87]. Early, authorities considered the incidence to be equal in females and males [88], but there is a slight female predominance in most prevalence studies [83]. A trend for increasing female predominance over calendar time has been reported in several regions [89,90]. In a recent meta-analysis, sex ratio decreased with increasing latitude [91] and a similar finding was seen within a single study in a relatively homogeneous population [92]. This may reflect a differential effect of latitude-related factors on MS risk by gender [83,92], or changes in gender-specific smoking habits [93]. In a recent study of the US military veteran population, MS incidence was three-fold higher in women than in men, and incidence rates for Blacks were higher than for Whites (Relative risk (RR) = 1.27, 95% confidence interval (CI) 1.16–1.39), over a 60-year time period [94]. Population studies further support the important influence of environmental factors in risk of MS. In a systematic review [95], two consistent patterns were apparent: migrants moving from a region of high MS risk to one of lower risk had a lower-than-expected MS prevalence, particularly when migration occurred before age 15 years; migrants moving from an area of lower risk to one of higher risk tended to retain the

lower MS risk of their country of origin, with no clear age-at-migration effect. More recent studies have largely confirmed these patterns [96,97]. A large number of aetiological factors have been identified to play a role in MS including genetic susceptibility, smoking [98], exposure to the Epstein-Barr virus (EBV) [99] and low exposure to sunlight (presumed to be mediated through vitamin D insufficiency) [100,101,102].

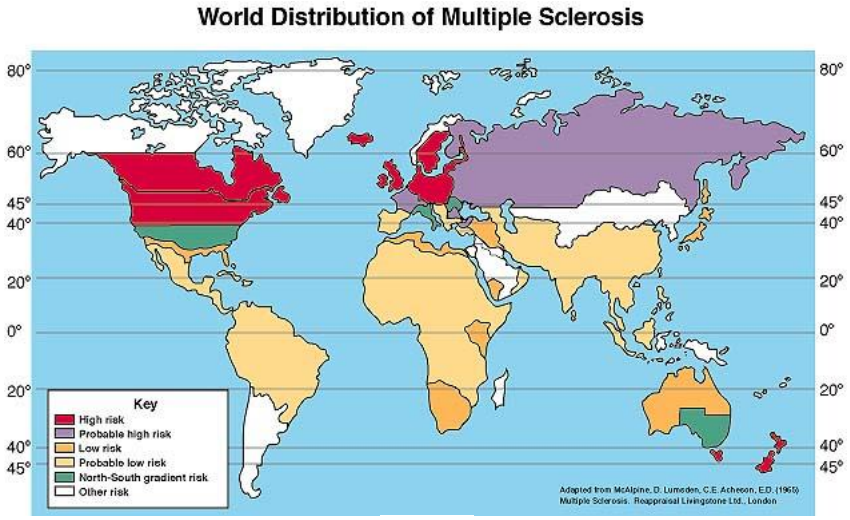

Fig. 4 msrc.co.uk

The causes of MS are mostly unknown, although twin and sibling pair studies point to a genetic component [103]. The concordance rate among identical twins is approximately 30%, [104,105] and the clinical course of MS among related individuals seems to be similar. However, there is a large environmental component to MS as well, complicating efforts to identify the genes responsible for increasing susceptibility and affecting clinical outcome.

The most promising candidate gene associated with MS is *HLA-DRB1*. Studies of the HLA chromosomal region consistently show evidence for a link to MS susceptibility. HLA proteins play an important role in immune recognition of self vs. non-self [105]. The **1501* allele of HLA is present in approximately 48% of MS patients, indicating that it is likely involved in the pathogenesis of the disease. The individual risk for developing MS is about twice as high in individuals who carry two copies of the **1501* allele. Interestingly, the HLA region is implicated in almost all autoimmune diseases [106].

Another promising candidate gene that may impact on the development of MS is the *Interleukin 7 Receptor α subunit* (*IL7Rα*). IL7Rα is involved in the homeostasis of the memory T-cell pool and in generation of autoreactive T cells [107]. For those carrying a variant form of *IL7Rα*, it is thought that there is an increase in the amount of soluble versus membrane-bound receptor, affecting signalling through the Interleukin pathway. Approximately 30% of MS cases may be explained by having the *IL7Rα* variant [106].

In addition to investigating the genetic control of the risk of developing MS, there is current investigation into the genetics of MS clinical outcome. MS clinical outcome is widely variable among patients. However, it has been observed that age at onset, disease course, and rate of acquisition of variability are similar in siblings and twins, suggesting a genetic component to phenotypic expression [103]. Several genes are being studied for their effects on the clinical outcome of MS.

Although genetic testing cannot yet accurately identify those at risk of developing MS, research is rapidly advancing. Genome-wide association studies are increasingly identifying candidate genes for a number of disorders including MS, [108] and it's possible that they may help to unravel the genetic mysteries of MS [109].

b) Pathogenesis

In the early MS disease process, T cells are primed in the periphery by antigen presenting dendritic cells, crucial regulators of specific immune responses. In the chronic phase, particularly oligodendrocytes, myelin and axons degenerate in the CNS, causing numerous symptoms often progressing into physical and cognitive disabilities. MS patients can be affected by a relapsing/remitting (RRMS) early form of the disease, but a large proportion of the patients soon evolves into primary (PPMS) and secondary progressive (SPMS) phases [110]. Although MS is in general regarded as a white matter (WM) disease, the incidence of demyelination and oligodendrocyte or neuron/axon injury are prominent and widespread in grey matter (GM) too [111]. MS lesions are abundant in cerebral cortex [112], where they constitute a significant

proportion of the overall pathology of the brain, with a particularly high prevalence of plaques being observed in progressive stages of the disease. In addition to changes to oligodendrocytes and

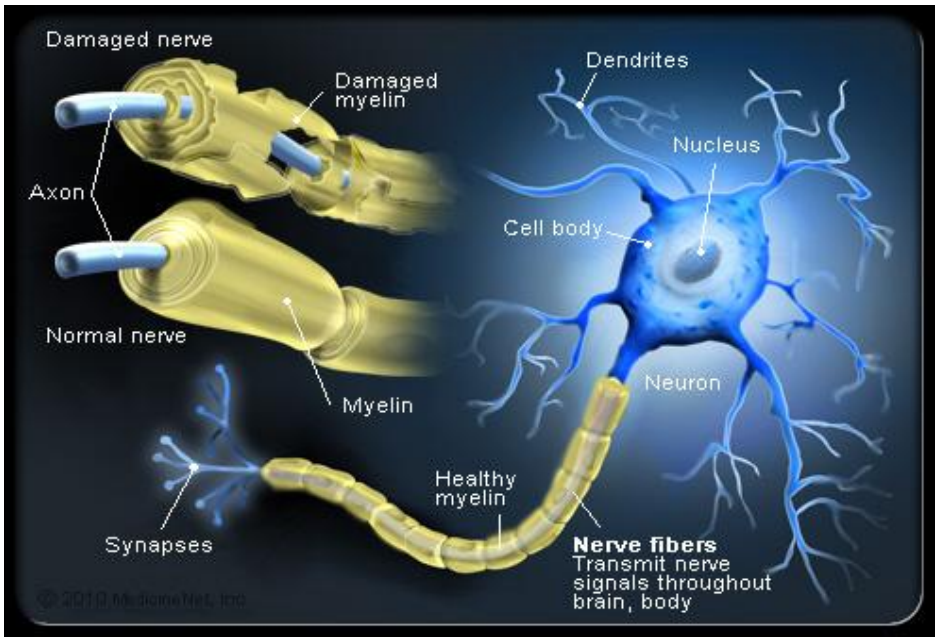

Fig. 5; 2010 Medicine Net, Inc

neurons (Fig. 5), current knowledge also emphasizes an important dual role for astrocytes and microglia in MS [113]. Astrocytes, for instance, can promote inflammation, damage to oligodendrocytes and axons, formation of the glial scar but, at the same time, can support migration, proliferation and differentiation of oligodendrocyte progenitors [114]. Likewise, microglia may play an essential causative function in MS pathogenesis, but also restore the damaged tissue [115,116]. As a result, all glial cells are likely to play significant roles in both the destructive and restorative phases of MS. Hence, a major challenge in MS research is to discern the conditions and factors that might contribute to the outcome of this unsteady equilibrium [117].

The pathological hallmarks of MS are inflammation, demyelination, remyelination, neurodegeneration and glial scar formation, which occur either focally or diffusely throughout the WM and GM in the brain and spinal cord [118]. These pathological features are present in both RRMS and SPMS, as well as in PPMS, although they vary over time both quantitatively and qualitatively between these three forms of MS and among individuals with the same form.

c) Inflammation

Inflammation is invariably present at all stages of MS [119]. Inflammatory lesions in patients with MS consist of perivascular and parenchymal infiltrates of lymphocytes and macrophages [120]. CD8+ T cells are present in greater numbers than are other T-cell subsets, B cells or plasma cells [119,121]. In active lesions, which dominate in the RRMS, low numbers of T cells are present at sites of initial tissue injury during the prephagocytic stage of lesion formation [122], and ongoing tissue injury is associated with infiltration of macrophages and/or activation of resident microglia [120]. Invasion of the majority of these inflammatory cells into the tissue occurs after the initial destruction of myelin [123,124]. This observation suggests that two different types of inflammation occur within active plaques: the initial response, consisting mainly of CD8+ T cells and abundant microglial activation; and secondary recruitment of T cells, B cells and macrophages as a consequence of myelin destruction. Inflammation in the RRMS is indicated by the infiltration of inflammatory cells into the CNS, resulting in profound damage to the blood–brain barrier (BBB), which has been demonstrated with gadolinium-enhanced magnetic resonance imaging of lesions [125,126].

In PPMS and SPMS, active demyelination and neurodegeneration are also invariably associated with inflammation [119]. However, the relationship between inflammation and damage to the BBB is less obvious than in RRMS [127]. First, mild BBB impairment, indicated pathologically by serum-protein leakage [127,128], can occur in conjunction with chronic lesions, irrespective of the presence or absence of inflammatory infiltrates [128,129]. However, the extent of BBB damage is too limited to be detected by gadolinium-enhanced MRI. The inflammatory process in the brains of patients with PPMS or SPMS also becomes, at least in part, dissociated from BBB damage, with the result that inflammatory infiltrates are frequently encountered around small veins and venules without evidence of loss of BBB integrity [127]. In the connective tissue spaces of the brain, such as the meninges and the large Virchow–Robin spaces, large aggregates of inflammatory cells have been observed, which display structural features of lymphatic follicles, such as T-cell-and-B-cell

germinal areas and the presence of follicular dendritic cells [130,131]. This observation demonstrates that as the disease progresses, inflammation becomes partly compartmentalized behind an apparently intact BBB.

d) Plaque formation

In the MS brain, plaques are present in the GM and WM at all stages of the disease [132] and focal plaques of demyelination are the diagnostic hallmark of MS pathology [133]. Traditionally, MS plaque classification has based on temporal progression, or stages, of inflammatory destruction. Accordingly, acute, chronic active, and chronic silent lesions are thought to occur along a continuous timeline, eventually producing the scarred and hardened areas within the CNS that can be appreciates grossly. The acute MS plaque represents the earliest stage of lesion formation. It is typified by robust inflammatory infiltration combined with demyelination distributed throughout the lesion. The constituents of immune cell influx centered around vessels (termed perivascular cuffing) include lymphocytes (predominantly T cells), monocytes and macrophages.

The chronic plaque is characterized by a region of hypocellularity with loss of myelin and glial scarring. In chronic active lesions, inflammation continues along the outer border with the histologic appearance comparable to acute lesions. Thus, borders of the chronic active plaque are populated with activated microglia and macrophages, vessels demonstrating perivascular cuffing, and reactive astrocytes. The core of the chronic plaque is typically hypocellular, though, and often contains thickened vessels with enlarged perivascular spaces. Chronic silent lesions are characterized by loss of the inflammatory traits along the border of chronic active lesions [134].

1.3.1 Autoimmune Animal Models

Experimental allergic encephalomyelitis (EAE) has received the most attention as a model of MS and is routinely used in testing therapeutic strategies for MS. This disease exhibits many clinical and histological features of MS and is caused by the induction of autoimmunity to antigens that are either naturally (typically myelin antigens) or artificially (such as implanted mycobacteria or

ovalbumin that, following peripheral sensitisation to these antigens, allows local targeted lesions to be developed) expressed in the CNS [135,136]. Following sensitisation to myelin antigens, animals develop disease, typified by limb paralysis (Fig.6). This is associated with BBB dysfunction, mononuclear cell infiltration into the CNS and conduction block resulting in impaired neurotransmission. This can occur in the absence of demyelination and highlights a misconception that clinical EAE is due to demyelination. In some models, disease is also associated with significant axonal loss, which is the underlying cause of persistent disability [135]. EAE is polygenic and multifactorial and both susceptibility and clinical course can vary depending on the immunising antigen (such as MBP, myelin basic protein, and PLP, myelin proteolipid protein) and/or the strain/species of animal being investigated [135,136]. For example, ABH and SJL mice develop relapsing EAE to disease induced by whole myelin, whereas C57BL/6 mice are resistant [135]. However, the discovery that myelin oligodendrocyte glycoprotein (MOG) can induce chronic paralytic EAE in the C57BL/6 mice has allowed the numerous gene-knockout mice bred on that background to be used to investigate EAE [135]. Although the rat has become a less frequently used EAE model, various active EAE models have been developed. Some display remarkable clinical and pathological similarity with MS, the rrMOG/ CFA (complete Freund's adjuvant)-induced EAE models in Dark Agouti (DA) and Brown Norway (BN) rats in particular [137,138]. DA rats develop mainly focal spinal cord and cerebellar lesions, as well as optic neuritis, where as BN rats develop a clinical picture reminiscent of neuromyelitis optica [139].

In LEWIS rats, fresh guinea pig spinal cord homogenate (GPSCH) emulsified in CFA is used to induce EAE. Rats with acute EAE suffered from quick, severe attacks with widespread inflammatory cells. No demyelination or astrocytic hyperplasia was found around the lesion [140].

Therefore, EAE is not a single model, but a number of models that have varying degrees of similarity to MS [135]. As such, a similar clinical phenotype may be achieved via different routes of genetic control and likewise suggests that there is likely to be some heterogeneity in the pathways leading to disease in MS [139].

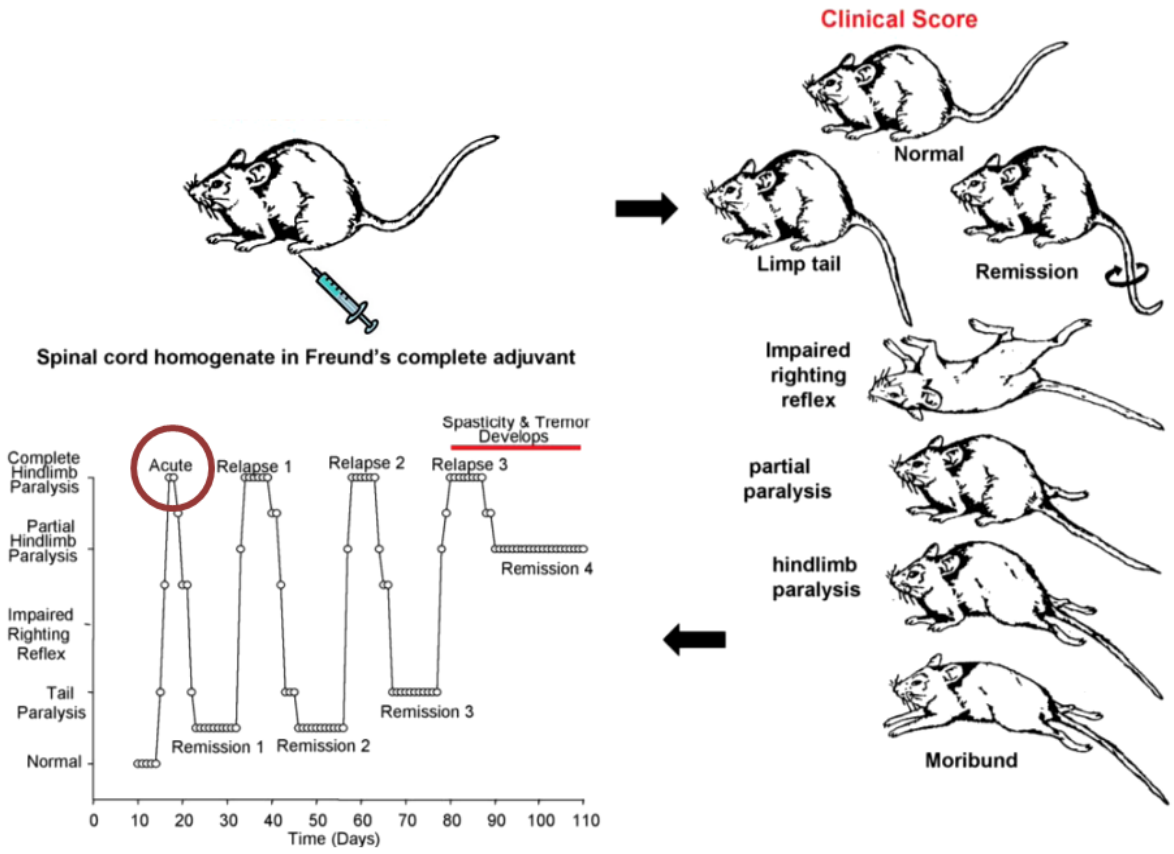

Fig. 6 Modify from Baker D. et al., 2007

1.3.2 Multiple Sclerosis and P2 receptors

Extracellular purine/pyrimidine nucleotides and nucleosides are among the most widespread exogenous signals playing important either detrimental or protective roles in neuron-to-glia and glia-to-glia communication, in the normal and injured brain [141,142]. However, not much is known regarding purinergic signalling and MS. For instance, not only ATP, but also adenosine can directly modulate migration, proliferation, and differentiation of oligodendrocyte progenitor cells (OPCs). Adenosine inhibits OPCs proliferation while promotes OPCs differentiation and myelination [143], and stimulates OPCs migration via A1A receptors [144]. ATP would instead trigger proliferation, migration, and differentiation of OPCs primarily via several different P2Y receptors [145,146,147], and activation of P2 receptors evokes Ca^{2+} signals in OPCs and oligodendrocytes in situ and in culture [146,147,148,149]. Thus, the general opinion is that axons

release adenosine and ATP during propagation of action potential, in order to control oligodendrocyte development, with an overriding role for adenosine in stimulating terminal differentiation, and for ATP in promoting myelination also via astroglial components [150].

Study on P2X receptors established that probably P2X4 subtype is involved in EAE pathology, being expressed by macrophages infiltrating in the brain and spinal cord from early and asymptomatic phase, to recovery phase of EAE. Moreover, the kinetics of accumulation of P2X4 receptor in macrophages are parallel to those of infiltration and disease severity, therefore suggesting a likely role for this receptor in immunoregulation during CNS inflammation [151]. In addition, by analyzing the distribution pattern of all P2 receptors in sections of cerebral cortex from post-mortem MS brains, a clear immunoreactive signal for P2X1 protein is found in blood vessels on cells of the haematopoietic origin; P2X2,4 receptors appear localized in GM neuronal nuclei; a strong signal for P2X3 protein is present only in degenerating cortical pyramidal neurons in GM, and for P2Y2,11 in the entire frontal cortex. P2Y6,14 immunoreactivities are instead very weak and localized to small areas. Finally, P2X6 and P2Y1 receptors seem absent from WM and GM MS frontal cortex, whereas P2X5, P2Y4,13 proteins could not be detected [152]. The metabotropic P2Y12 receptor is instead abundantly expressed in myelin and interlaminar astrocytes, but absent from protoplasmic astrocytes of the deeper cortical layers, absent from microglia/macrophages and from intact demyelinated axons in MS brain. Moreover, a decreased P2Y12 protein in proximity to the lesions is directly correlated with the extent of demyelination found in all types of GM cortical plaques and subcortical WM. It was hence suggested that loss of purinergic P2Y12 receptor might be detrimental to tissue integrity in MS [152]. This is still to be confirmed in the EAE mouse model, where the P2Y12 receptor is shown to colocalize with MBP in spinal cord sacral sections [117].

A recent work has hypothesized that extracellular ATP might directly contribute to MS lesion-associated release of IL-1β via P2X7 receptor-dependent induction of cyclooxygenase-2 protein and downstream pathogenic mediators [153].

Matute and co-workers [154], have shown that oligodendrocytes and myelin indeed express functional P2X7R mediating cell death *in vitro* and *in vivo*. Activation of P2X7R, moreover, contributes to tissue damage in EAE. Finally, P2X7R blockade prevents oligodendrocyte excitotoxicity and ameliorates EAE and receptor expression is even increased in MS human tissue before lesion formation [154]. It was also demonstrated that mice deficient in P2X7R function are less susceptible to EAE than wild-type mice, also showing reduced CNS inflammation [155]. However, authors have also reported that P2X7R knockdown displays a reduction in IL-1 and -6, with concomitant decrease in lymphocytic apoptosis and exacerbation of the EAE phenotype [156]. Moreover, monocytes from both MS and control subjects express P2X7R, IL-1β and CD39, and glatiramer acetate (an immunomodulator drug currently used to treat MS) seems to interfere with such expression [157,117].

2. Aim of the study

By using both the EAE rat model and MS autoptic cortical tissue and peripheral blood mononuclear cells (PBMCs) from patients and healthy donors, this thesis aims to further examine the potential involvement of P2X7R in MS pathogenesis, and to possibly understand if activation of this receptor subtype might be beneficial or detrimental to the onset and progression of MS. Since it's known that P2X7R is expressed on cells of hematopoietic lineage, as well as on CNS cells, and its functional role in MS pathogenesis is marginally defined or even controversial in some cases, we will perform a comparative analysis among different tissues and cell phenotypes by analyzing, in particular, those cell types having a major role in the inflammatory MS reaction, such as astrocytes, microglia and monocytes present either in the CNS or peripheral blood.

MS lesions are known to be abundant in the cerebral cortex, where they constitute a significant proportion of the overall pathology of the brain, with a predominantly high prevalence of plaques being observed in progressive stages of the disease. Moreover, although MS is still regarded as a

WM disease, the incidence of neuron/axon injury is prominent and widespread in GM. For all these reasons, in our work we will analyze several different brain areas where the expression of the P2X7R is still not investigated, but we will concentrate our studies mainly on cortical tissue from patients affects by primary and secondary progressive stages of the disease. By comparing the results obtained in patients with those in the EAE rat model exemplifying a condition of acute phase of MS, we will be able to track the state of P2X7R activation throughout the major symptomatic phases of MS.

3. Materials and methods

EAE rat model . Pathogen-free, female Lewis rats weighting approximately 160 g (6 weeks old) were purchased from Charles River (Como, Italy), housed in group of two per Plexiglas cage (18 x 30 x 24 cm), and allowed free access to food and water. All animal procedures have been performed according to the European Guidelines for the use of animals in research (86/609/CEE) and the requirements of Italian laws (D.L. 116/92). The ethical procedure has been approved by the Animal Welfare Office, Department of Public Health and Veterinary, Nutrition and Food Safety, General Management of Animal Care and Veterinary Drugs of the Italian Ministry of Health. All efforts were made to minimize animal suffering and to use the number of animals only necessary to produce reliable results.

Eight female Lewis rats were deeply anaesthetized and injected in each hind paw with 100 µl of a medium containing 0.15 g/ml Guinea Pig Spinal Cord tissue in saline (0.9% NaCl) and complete Freund's adjuvant (CFA, Sigma), 50% vol/vol, to which 5 mg /ml heat-inactivated Mycobacterium tuberculosis (Difco H37Ra) were added [158]. Three uninjected rats were used as controls and six CFA-injected rats were used as control of inflammation.

Starting at day 4 post-injection (dpi), all animals were daily weighed, assessed for clinical signs of disease and graded according to the following described criteria: 0 = no clinical signs; 1 = loss of tail tonus; 2 = weakness in one or both hind legs or middle paresis; 3 = severe paresis or paralysis of

both hind legs; 4 = severe paralysis of complete lower part of the body; and 5 = death due to aggressive EAE. Scores 3 and 4 were often accompanied by urinary and fecal incontinence [159].

In order to investigate the differences in stress response that could affect depression/anxiety levels due to EAE induction, animals were subjected to the forced-swim test (FST) at 13 dpi, following methods previously described (43). Each rat was individually placed in a glass cylinder (20 x 50 high cm) containing water at 25 ± 1°C. After 9 min, the swimming test session was carried out during the light phase of L/D cycle. Animals were tested under indirect dim light. At the end of each session, animals were towel dried and transferred into a heated chamber (37 ± 1°C) for a 20 min warm-up period. Each test session was analyzed by a highly trained observer blind to the treatment, in order to score the latency to the first floating episode as an index of depression/anxiety condition and, the total immobility time. A rat was judged to be immobile when it ceased struggling and remained motionless , i.e. floating in the water making only movements necessary to keep its head above water [160].

Tissue preparation. All rats were sacrificed at 15 dpi. Brains (3 CFA and 4 EAE) were quickly removed from the skull and different tissues isolated and stored at -70°C until used for protein extraction. In parallel, control (n=3), CFA(n=3) and EAE (n=4) rats were deeply anesthetized with Chloralium Hydrate (400mg/Kg body weight) and perfused with 4% paraformaldehyde in 0.1 M phosphate buffer. Brains were removed, postfixed with 4% paraformaldehyde, cryoprotected with 30% sucrose in 0.1 M phosphate buffer saline (PBS), and used for immunohistochemical analysis.

Human brain tissue . Brain tissue was collected postmortem with fully informed consent from both donors and close relatives by UK Multiple Sclerosis Tissue Bank at Imperial College, London. Procedures for retrieval, processing, and storage have gained ethical approval from all appropriate committees. The brain tissues analyzed in this study were from 6 neuropathologically confirmed cases of MS, with different disease courses (PPMS/SPMS), ages (range 34-80 years), durations (range 11-50 years) and causes of death. Analysis was performed also on samples from 2 patients who died due to non neurological diseases. Cerebral hemispheres were fixed with 4%

paraformaldehyde for about 2 weeks, coronally sliced, and blocked. Individual blocks were cryoprotected in 30% sucrose for 1 week and frozen by immersion in isopentane precooled on a bed of dry ice. Frozen tissue blocks were stored at –80°C.

Immunohistochemistry. After quenching of endogenous peroxidase by a 10-min incubation with 5% H2O2 in 5% methanol in PBS (human sections, 30-40 μm thick) and with 0,3% H2O2 in PBS (rat sections, 40μm thick), the sections were incubated for 24-48 h in PBS-0.3% Triton X-100 and 2% normal donkey serum (NDS) at 4°C, with primary antisera/antibodies, as specified in Tables 1-2. Sections were then incubated either with biotinylated donkey anti-mouse, biotinylated donkey anti-rabbit (Jackson Immunoresearch Laboratories, West Grove, PA), followed by avidin-biotin-peroxidase reactions (Vectastain, ABC kit, Vector, Burlingame, CA), using 3,3'-diaminobenzidine (Sigma Aldrich) as a chromogen. Sections were mounted on poly-lysine slides and air dried for at least 24 h. The histological preparations were examined using an Axioskop 2 light microscope (Zeiss, Iena, Germany). Images were taken with Neurolucida software (MBF Bioscience, USA).

Double and Triple Immunofluorescence. Human/rat sections (30-40 μm thick) were processed for double and triple immunofluorescence studies. Nonspecific binding sites were blocked with 10% NDS in 0.3% Triton X-100 in PBS, for 1 h at room temperature. The sections were incubated with a mixture of primary antisera/antibodies (Tables 1- 2) in 0.3% Triton X-100 and 2% NDS in PBS, for 24-48 h at 4°C. The secondary antibodies used for double labeling were Cy3-conjugated donkey anti-rabbit immunoglobulin G (IgG) (1:100, Jackson Immunoresearch, red immunofluorescence), Alexa Fluor® 488-AffiniPure donkey anti-mouse IgG (1:100, Jackson Immunoresearch, green immunofluorescence). Moreover, in the case of biotinylated primary antibodies, Cy2- or Cy5-Streptavidin coniugated secondary antibodies (1:200, Invitrogen; 1:200, Jackson Immunoresearch) was used. For the third color labeling, Cy5-conjugated donkey anti-mouse IgG (1:100, Jackson Immunoresearch, blue immunofluorescence) was used. The sections were washed in PBS 3 times for 5 min each and then incubated in a solution containing a mixture of the secondary antibodies in

0.3% Triton X-100 and 2% NDS in PBS, for 3 h at room temperature. After rinsing, the sections were mounted on slide glasses, air dried, coverslipped with gel/mount antifading medium (Sigma).

Confocal Microscopy. Double or triple immunofluorescences were performed by means of a confocal laser scanning microscope (Zeiss, LSM700; Germany) equipped with four laser lines: 405nm, 488nm, 561nm and 639nm. The brightness and contrast of the digital images are adjusted using the Zen software. Signal specificity was positively proved by performing confocal analysis in the absence of the primary antibodies/antisera, but in the presence of either anti-rabbit or anti-mouse secondary antibodies. Specificity was further confirmed for the P2X7R antiserum by performing immunoreactions in the simultaneous presence of the P2X7R neutralizing immunogenic peptide. The polyclonal P2X7R antiserum used in this study was raised against a highly purified peptide (identity confirmed by mass spectrography and aminoacid analysis, as indicated in the certificate of analysis provided by the manufacturer), corresponding to an epitope not present in any other known protein.

Human Antibodies (table 1)

Antigen	Clone	Target	Dilution	Source
MBP	**2**	**Mature oligodendrocytes/myelin**	**1:100**	**Chemicon**
Cd11b	**5C6**	**Microglia/Macrophages**	**1:200**	**Abd serotec**
CD45	**61D3**	**Leukocyte**	**1:100**	**Dako**
CD14 biot	**T29/33**	**Monocytes**	**1:100**	**eBioscience**
HLA- DP, DQ, DR (MHC II)	**CR3/43**	**Macrophages/Microglia**	**1:100**	**Dako**
CD68	**EBM11**	**Macrophages/Microglia**	**1:100**	**Dako**
GFAP	**6F2**	**Astrocytes**	**1:400**	**Serotec**
P2X7 receptor	**Polyclonal**	**P2X7 receptor**	**1:500**	**Alomone**

Rat Antibodies (table 2)

Antigen	Clone	Target	Dilution	Source
MBP	**2**	**Mature oligodendrocytes/myelin**	**1:100**	**Chemicon**
Cd11b	**OX-42**	**Microglia/ Macrophages**	**1:200**	**Serotec**
CD68	**ED1**	**Macrophages/ Microglia**	**1:100**	**Santa Cruz**
GFAP	**6F2**	**Astrocytes**	**1:400**	**Serotec**
P2X7 receptor	**Polyclonal**	**P2X7 receptor**	**1:200**	**Alomone**

Protein Extraction and Western Blotting. Rat tissues were homogenized with ultrasonication in RIPA buffer (50 mM tris, pH7.5; 150 mM NaCl; 5 mM EDTA; 1% Triton X-100; 0.1% SDS; 0,5% DOC (Sodium deoxycholate; 1mM PMSF; 1µg/ml leupeptin), centrifuged at 4° C for 20 min at 13000 rpm, then supernatant was stored at -20°C. Protein quantification was performed from the supernatants by BCA Protein Assay (Biorad, Milan, Italy). Samples (30 µg of total protein) were dissolved in loading buffer (0.1 M Tris–HCl buffer, pH 6.8, containing 0.2 M dithiothreitol, DTT, 4% sodium-dodecil-phosphate, SDS, 20% glycerol, and 0.1% bromophenol blue), separated by 10% or 12% polyacrylamide gel electrophoresis (SDS-PAGE), and transferred to nitrocellulose Hybond-C-extra membranes (Amersham Biosciences, Cologno Monzese, Italy).

Human snap-frozen blocks from 4 cases of SPMS were homogenized in Ripa buffer (1% Nonidet P-40, 0.5% sodium deoxycholate, 0.1% SDS in PBS, containing protease inhibitors). After a short sonication, the homogenates were incubated on ice for 1 h and centrifuged at 14,000 rpm for 10 min at 4 C. Protein quantification was performed from the supernatants by Bradford colorimetric assay (Biorad). Proteins (60 µg) were separated by electrophoresis on 12% SDS-PAGE and transferred to nitrocellulose Hybond-C-extra membranes (Amersham Biosciences).

The filters were prewetted in 2% blocking agent in TBS-T (10 mM Tris pH 8,150 mM NaCl, and 0.1% Tween 20) and hybridized overnight with P2X7 antisera (1:500).

Incubations of P2X7 antisera were performed either in the absence or in the presence of the neutralizing immunogenic peptides used in a 1:1 protein ratio. The antisera were immunodetected with an anti-rabbit horse radish peroxidase-conjugated antibody (1:2500) and developed by enhanced chemiluminescence (Amersham Biosciences), using Kodak Image Station (KDS IS440CF).

***Flow cytometry analysis*.** PBMCs were obtained from 20 ml of freshly venous blood from 4 relapsing MS patients (MS acute) and 10 remitting MS patients (MS stable). Blood was diluted 1:2 with PBS pH 7.2, and PBMCs were isolated from buffy coats by a density gradient centrifugation over a Ficoll-Hypaque (Ficoll-Paque PLUS, GE Healthcare). Cells were stained with pre-titrated Abs, to evaluate the expression of P2X7R within CD14+ cells. Briefly, PBMCs ($1x10^6$) were incubated with anti-P2X7R (1:100; Alomone) for 30 min at 4°C. Cells were washed and stained with goat anti-rabbit Alexa Fluor 488-conjugated antibody (1:100; Invitrogen), 30 min 4°C. Cells were washed and stained with anti-CD14 PE (1:200; Dako) and LiveDead Fixable Aqua Dead Cell Stain Kit (1:200, Invitrogen), 30 min 4°C.

Moreover, monocytes from healthy donors PBMCs, were isolated by using a Magnetic Separation with Negative Selection Columns (Miltenyi Biotec). This population of purified monocytes ($6x10^6$) were cultured in RPMI 1640 with stable L-Glutamine, 50U/ml penicillin and 50 μg/ml streptomycin and serum-free and were dispensed in a 96-well plates. Then, monocytes were stimulated with or without LPS (100ng/ml, Sigma) and BzATP (250 μM, Sigma) for 4 h (T4) and 24 h (T24) at 37°C in a 5% CO_2 environment to evaluate the P2X7R expression. After the treatments, monocytes were incubated with anti-P2X7R (1:100) for 30 min at 4°C. Then cells were washed and stained with goat anti-rabbit Alexa Fluor 488-conjugated antibody (1:100), 30 min 4°C, subsequently, cells were washed and stained with anti-CD14 PE (1:200) and LiveDead (1:200), 30 min 4°C.

FACS (Fluorescence-activated cell sorting; FACS CyAn, Beckman Coulter) analysis, was used to evaluate the expression of P2X7R coupled with advanced flow cytometry software (FlowJo, Tree Star, Ashaland, OR).

RT-PCR assay

RNA isolation. Total RNA was isolated using Trizol (*Invitrogen*) reagent according to the manufacture's procedure. Briefly, PBMCs of healthy donors or MS brain cortex (10 mg) were homogenized in 800 µl Trizol reagent. After incubation at room temperature for 5 min, cells were centrifuged (12,000 x g) for 15 min at 4°C to remove excess lipids. Chloroform (100 µl) was added to supernatant, vortexed, and centrifuged (12,000 x g) for 15 min at 4°C to achieve phase separation of nucleic acids. Isopropyl alcohol (250 µl) was added at the acqueous phase to precipitate nucleic acids. Samples were vortexed (1 min) and incubated at room temperature for 10 min, followed by centrifugation (12,000 x g) for 10 min at 4°C. Nucleic acids pellet was washed twice in 75% ethanol (500 µl) and centrifuged (7500 x g) for 5 min at 4°C. UV spectrophotometric analysis of nucleic acids was performed by Nanodrop spectrophotometer at 260 nm to determine concentration. The 260:280 absorbancy ratio was used to assess nucleic acids purifity.

cDNA synthesis. Total RNA was reverse transcribed into cDNA using the Enhanced Avian HS RT-PCR kit (Sigma Aldrich). RNA (1 µg) was incubated for 10 min at 70°C in a total reaction volume of 10 µl containing random nonamers (2.5 µmol) and dNTPs (500 µM). Samples were chilled on ice for 1 min. A cDNA synthesis buffer was added to the reaction with Reverse Transcriptase enzyme (200 U of AMV-RT) and RNase Inhibitor (1U/µl). Retrotranscription mix was incubated at 50 °C for 60 min and then de-activated by heating at 70°C for 15 min. To remove RNA complementary to cDNA, *E.Coli* RNase H (2U) was added, followed by incubation at 37°C for 20 min.

PCR. PCR amplification was performed on all samples using the following primers: 1. *P2X7forward* 5'tgtgctcatcaagaacaatatcgact 3', *P2X7reverse* 5'ccacaaaggacacatactttaatgtcg 3'designed on human P2X7 sequence. Primers were tested for sequence specificity using ClustalW Alignment Tool (www.ebi.ac.uk/clustalw; EMBL-EBI) and Primer-BLAST (http://www.ncbi.nlm.nih.gov/tools/primer-blast). PCR was performed using JumpStart AccuTaqLA DNA polymerase mix (Sigma Aldrich). PCR cycling conditions consisted of step of 2 min 94°C, 38 cycles of denaturation , amplification, extention (95°C 30 sec; 60 °C 30 sec; 72°C 1

min), 7 min 72 °C. Products were analyzed by agarose gel electrophoresis using Ethidium Bromide to visualize DNA. Acquisition of gels was done using Kodak Image Station.

Statistical analysis. Western blotting and FACS data are presented as mean ± standard error of the mean. Statistical differences were verified by Graph Pad Prism's t test; $*p < 0.05$ was considered significant. Clinical EAE scores and body weight gain trend are compared between treatment groups by the analysis of variance (ANOVA) for repeated measures at each dpi. Difference between groups was determined by Tukey-Kramer multi-comparison; $*p < 0.05$ was considered statistically significant.

4. Results

4.1 Use of the Lewis rat model of EAE.

In order to investigate the role of P2X7R in MS, especially on cells of hematopoietic lineage and CNS participating to the inflammatory reaction, we first adopted the EAE acute Lewis rat model, according to Beeton et al., 2007 [161]. This model with its inflammatory features, is one of the most commonly used animal model for studying the pathogenesis of human MS.

Briefly, we injected female Lewis rats with either CFA (not causing symptoms and MS-like pathogenesis) or with the immunogenic EAE mixture (guinea pig spinal cord, complete Freund's adjuvant and heat-inactivated mycobacterium tuberculosis) and kept the animals for 15 dpi, until they were sacrificed and brain excised for analysis. Physiological parameters (body weight) and behavioral scores were analyzed every other day starting after recovery of the animals from the immunogenic injection (4 dpi). Following this protocol, we confirmed only about 20% reduction of body weight at 14 dpi, with respect to CFA and control animals (**Fig. 7**).

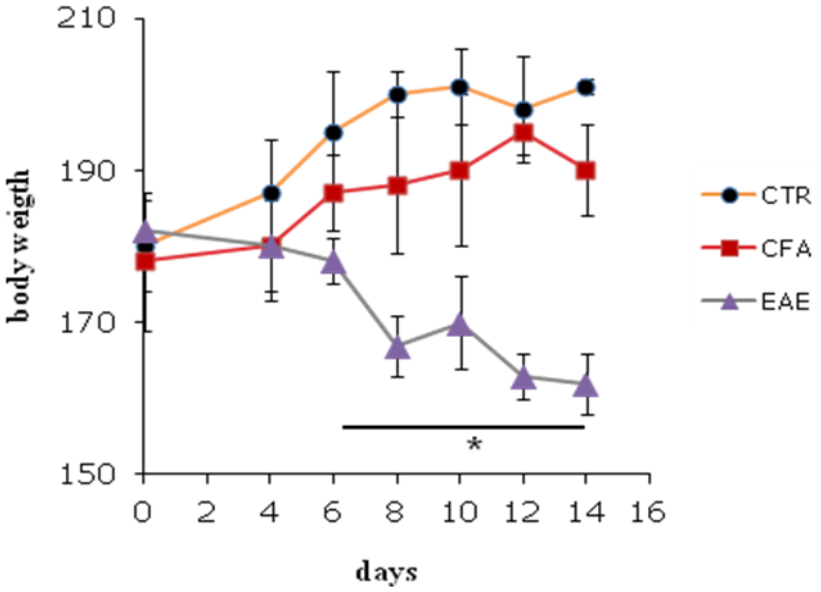

Fig. 7 Weight trend. Body weight of EAE compared to CFA and CTRL rats. EAE rats showed decreased body weight starting at 6 dpi after EAE induction, with respect to CTRL and CFA animals. Statistically significant differences were observed between groups. Anova test for repeated measure, *p<0,05.

Moreover, EAE rats started to manifest ataxia at 6 dpi, while this became significant only at 8 dpi (average score = 2.5±0.5) and reached complete limb paralysis at 14 dpi. EAE rats were then sacrificed when they reached severe clinical symptoms (15 dpi). With the exception of a local paw inflammation occurring within the first days after CFA or immunogenic EAE mixture inoculation and likely associated to partial wedding gait, no signs of ataxia or paralysis were reported in CFA rats (**Fig. 8**).

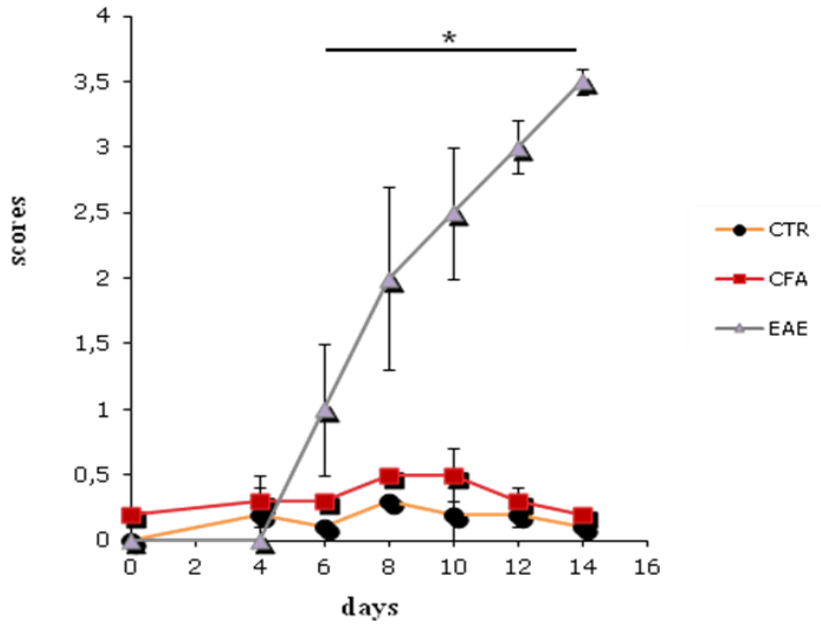

Fig. 8 Behavioral scores trend. Worsened general conditions were observed in EAE rats with respect to CFA and Control animals. EAE showed ataxia at 6 dpi, with total paralysis obtained at 14 dpi. Anova test for repeated measure (*p<0,05).

We also performed Forced Swim Test (FST) at 13 dpi, in order to monitor the anxiety/depression levels of all animals. FST analysis showed that the CFA group was in part affected, likely due to CFA injection, the EAE group showed a more significant increase of anxiety/depression by reducing the first floating latency time at about 3 minutes, with respect to about 6 minutes of CTRL and about 4 minutes of CFA group (**Fig. 9**).

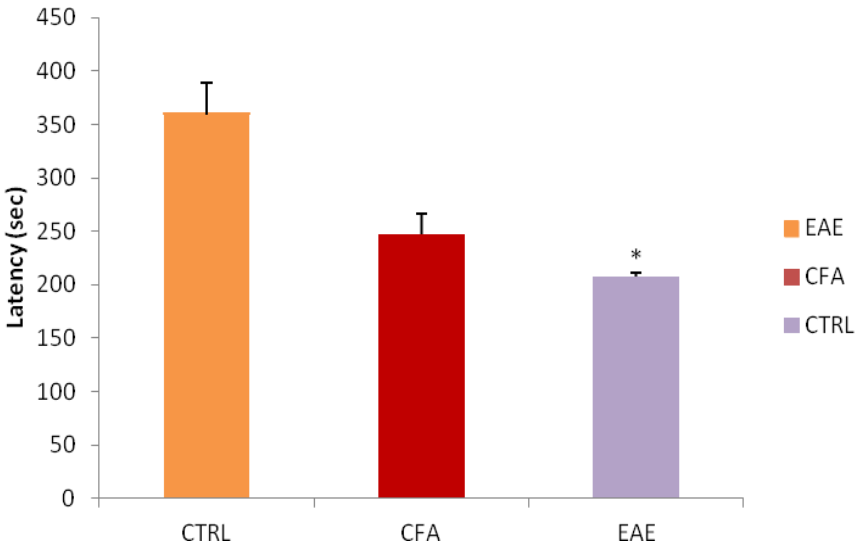

Fig. 9 Forced swim test analysis. Increased anxiety was present in EAE rats, with respect to CTRL and CFA. The first floating latency reduction also observed in CFA rats might be due to CFA injection. *p<0,05.

4.2 P2X7R protein is present in brain of control and EAE Lewis rat.

In order to investigate if P2X7R is expressed in EAE brain tissue in concomitance with the insurgence of EAE behavioral impairment and increased anxiety, we performed Western blot comparative analysis of brain tissue from Lewis rat injected with either CFA or immunogenic EAE mixture. Four female Lewis rats were deeply anaesthetized and injected with EAE mixture, and three CFA-injected rats were used as controls. All rats were sacrificed at 15 dpi. Brains were quickly removed from the skull and different tissues (frontal cortex, striatum, hippocampus, septum, cerebellum and spinal cord) isolated and stored at -70°C, until used for protein extraction and Western blotting.

Under these conditions, the P2X7R was recognized as a single specific protein band of about 75 kDa in frontal cortex, striatum, hippocampus, septum, cerebellum and spinal cord, both in EAE and CFA animals (**Fig. 10**). P2X7R protein expression was observed in all analyzed tissues although it

did not appeared significantly up regulated in EAE, with respect to CFA samples, with the only exception of the striatum.

C= CFA
E= EAE

Frontal cortex

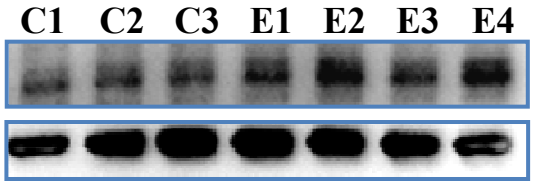

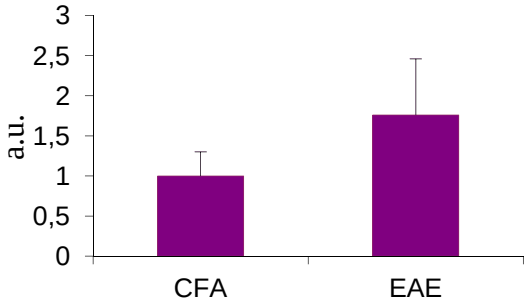

Spinal Cord

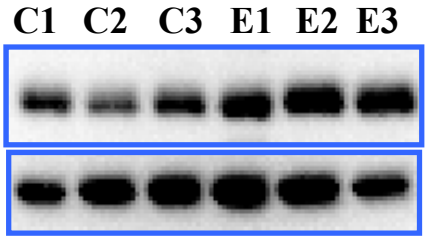

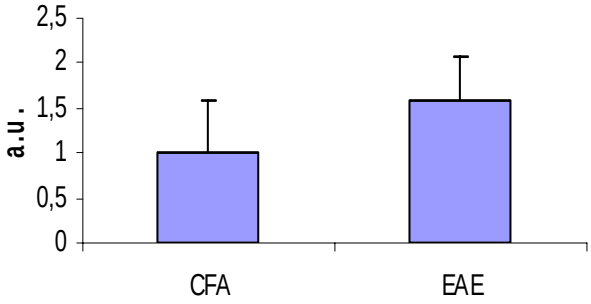

Striatum

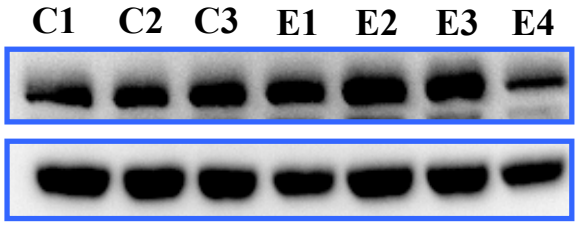

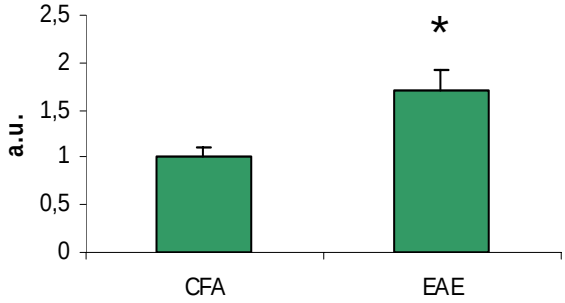

Hippocampus

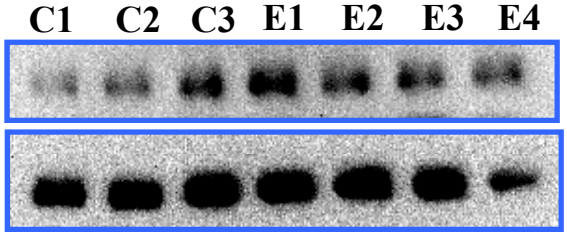

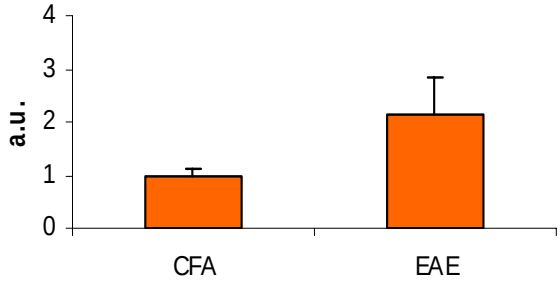

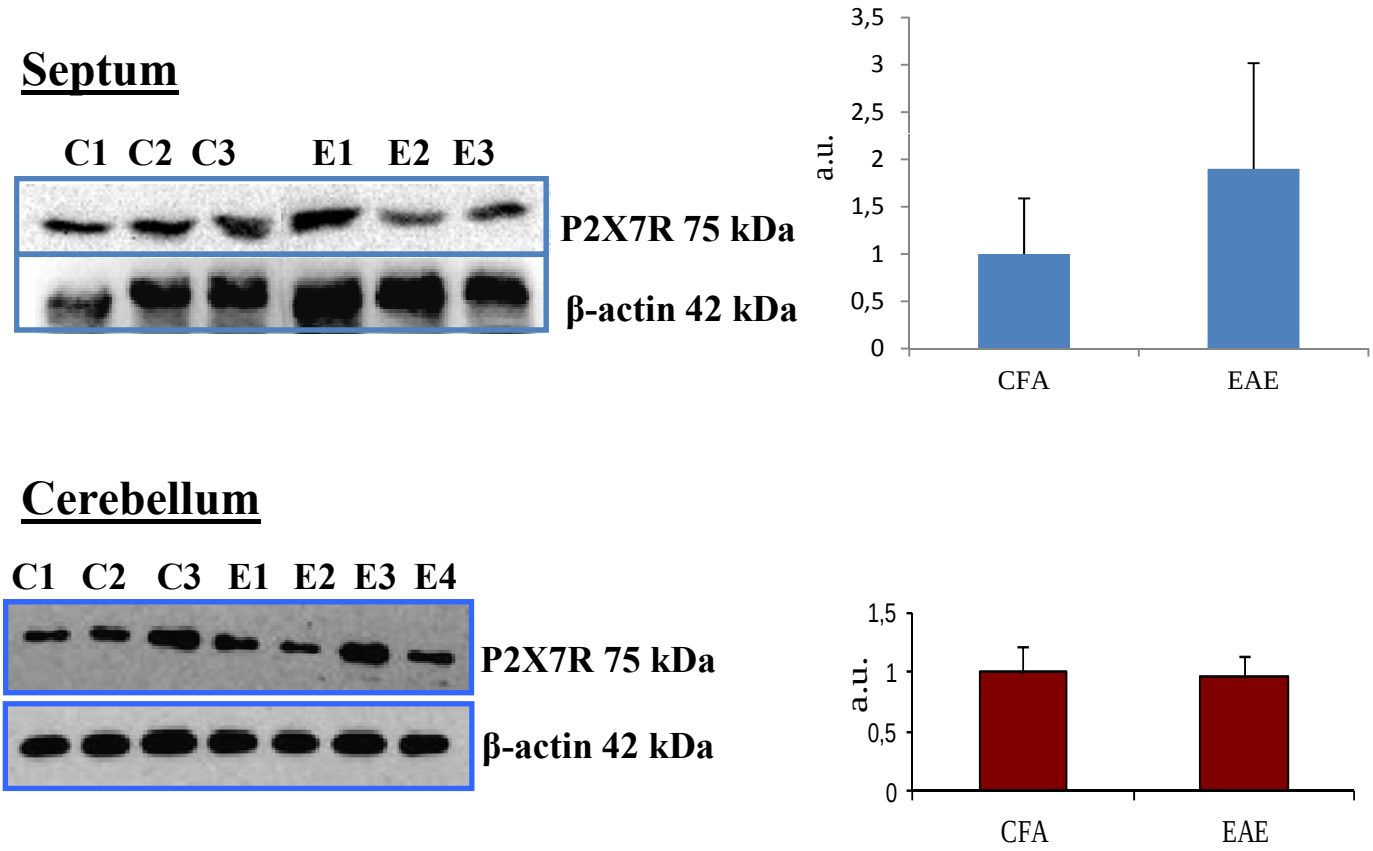

Fig. 10. P2X7R is present in brain extracts from control and EAE Lewis rat.
Western blot analysis of P2X7R protein demonstrates that the receptor is present in frontal cortex, spinal cord, striatum, hippocampus, septum and cerebellum in CFA and EAE rat brain tissue. Molecular mass of 75 kDa for P2X7R is indicated. *p<0.05.
a.u.: arbitrary units.

4.3 Gliosis in the EAE rat model.

Based on previous works [162] establishing that EAE animals are characterized by microglia activation, gliosis and lymphocytic infiltration, we studied these same parameters in our EAE tissues, with respect to CFA. We performed both immunohistochemistry and immunofluorescence confocal analysis with GFAP (glial fibrillary acidic protein), a marker for astrocyte, and Cd11b, a marker for microglia/macrophages, and analyzed particularly the septum, corpus callosum, cerebellum, striatum and cortex (Table 2). We identified sparse areas of gliosis in all tissues and found increased GFAP and Cd11b immunostaining in EAE, compared to CFA. As exemplified particularly in septum with GFAP, we observed more abundant and fibrous astrocytes occupying all the parenchyma in EAE tissue, with respect to CFA (**Fig. 11**, see GFAP-positive brown cells in A, and green cells in B). However, colocalization was not found for P2X7R and GFAP in all brain areas analyzed, and in either CFA or EAE tissues (data no shown).

Moreover, as exemplified particularly in corpus callosum with Cd11b, we observed an increased presence of ramified microglia in EAE tissue compared to CFA (**Fig. 12 A**, Cd11b-positive microglia cells are shown in brown, arrows). In cerebellum instead, by confocal analysis we showed that while microglia appeared with typical ramified cell bodies in a resting/surveilling condition and was uniformly dispersed in all the parenchyma of CFA tissue, in EAE animals microglia increased in number, acquired a roundish/ amoeboid morphology, and became highly abundant and concentrated in proximity of blood vessels (**Fig. 12 B**, see Cd11b positive microglia cells in green).

In order to localize the presence of P2X7R at the cellular level in Lewis rat EAE brain, we then performed double-immunofluorescence confocal analysis in cortex, corpus callosum, striatum, septum and cerebellum. As exemplified in the cerebellum (**Fig. 13)**, while Cd11b (in green) is labeling resting microglia uniformly distributed throughout the cerebellar parenchyma in CFA animals, induction of EAE caused disappearance of resting microglia and formation of Cd11b-positive patches of activated microglia localized especially near the blood vessels and staining microglia membranes. We found the presence of P2X7R (in red) only in rare resting microglia cells

in CFA animals, and in more abundant Cd11b-positive cells in proximity of blood vessels in EAE cerebellum. Cd11b immunostaining moreover colocalized with P2X7R immunostaining (in yellow) on both resting and roundish microglia, although not all Cd11b-positive cells expressed P2X7R protein in either CFA or EAE tissue. These results were similarly confirmed in cortex, corpus callosum, striatum, cerebellum and septum (data no shown).

In summary, from analysis of P2X7R in Lewis rat EAE model, we established that the receptor is present in extracts from selected brain areas (cortex, striatum, hippocampus, septum, cerebellum and spinal cord) although its expression is apparently not modulated after EAE induction. At the cellular level, P2X7R is found to colocalize only with microglia/macrophages present in the resting/surveilling state in CFA animals, and in the activated state in proximity of blood vessels in EAE animals. In all brain tissue analyzed, P2X7R was never demonstrated to colocalize with GFAP immunopositive signal (data not shown).

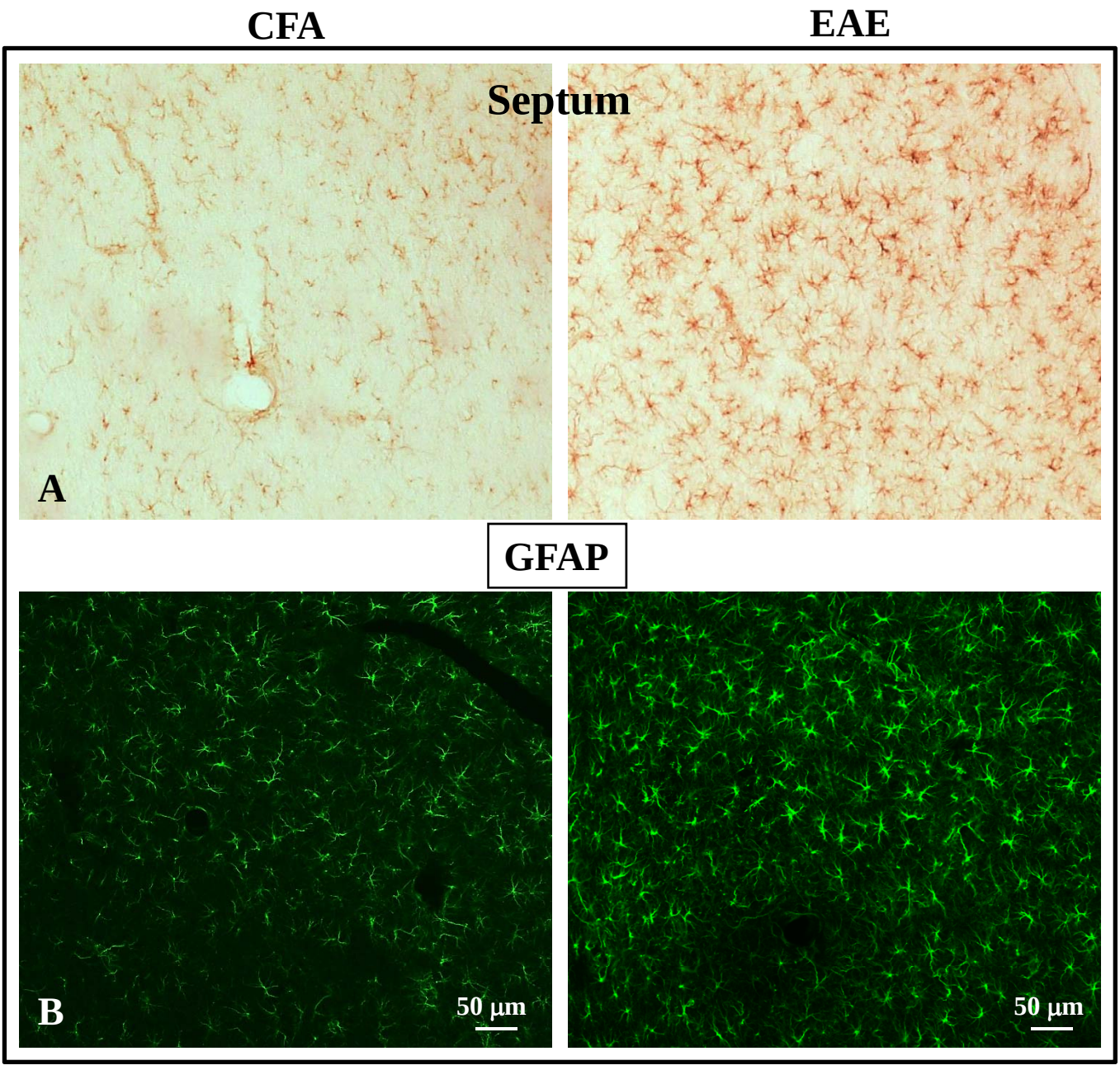

Fig. 11. Gliosis in the EAE rat model. Immunohistochemistry and immunofluorescence analysis shows increased astrogliosis in EAE septum with respect to CFA (GFAP-positive astrocytes are shown as brown in **A**, and green in **B**). The same condition is also verified in cortex, corpus callosum, striatum and cerebellum (data no shown). Scale bar = 50 μm, in **B**.

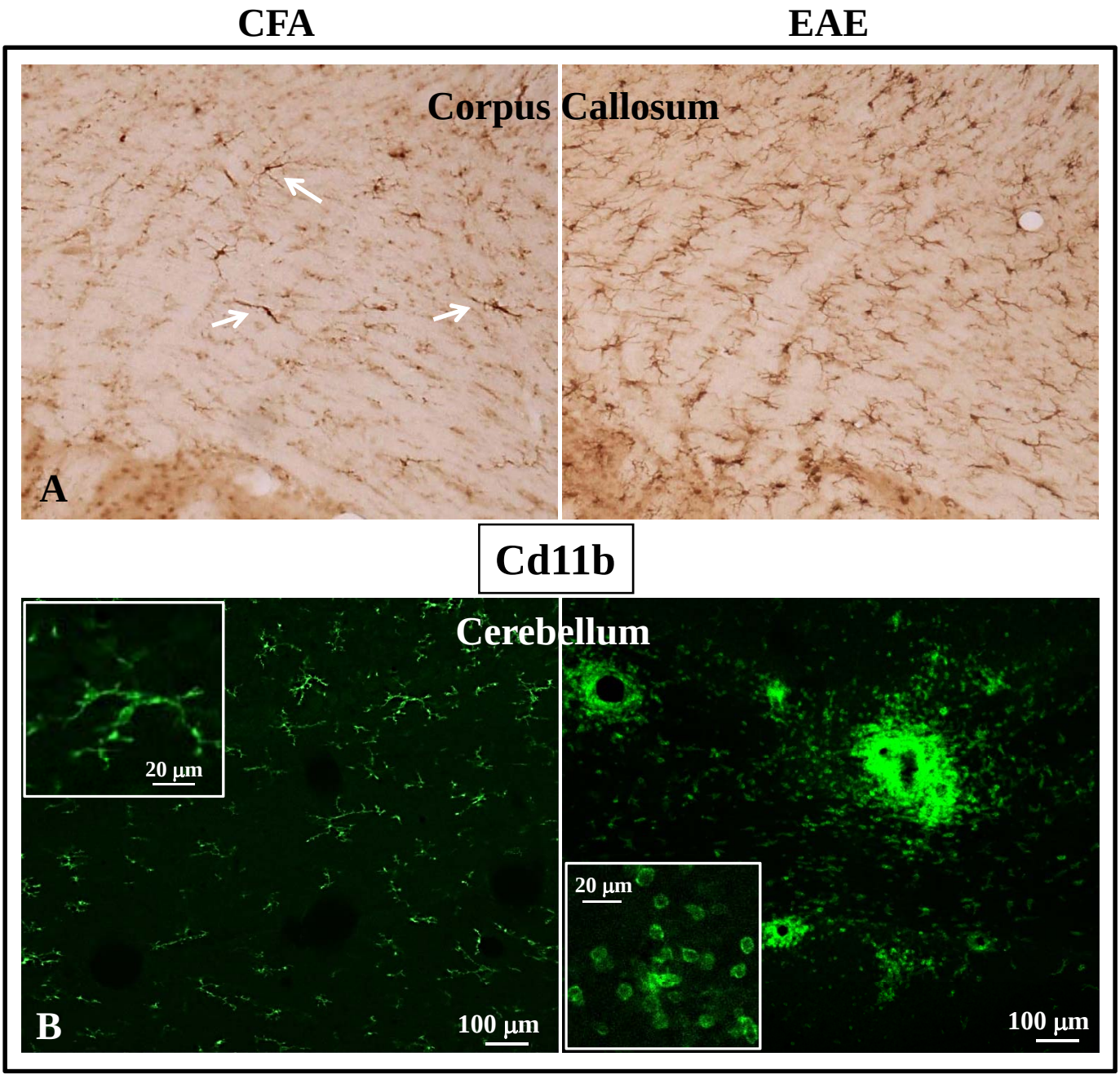

Fig. 12. Microgliosis in the EAE rat model. A, immunohistochemistry analysis shows increased microgliosis in EAE corpus callosum with respect to CFA (Cd11b-positive microglia cells are shown as brown, arrows). **B**, immunofluorescence analyses shows increased microgliosis in EAE cerebellum with respect to CFA, mainly near blood vessels (Cd11b-positive microglia cells are shown as green). Scale bar = 100 µm in **B**. Insets in B show microglial cells at higher magnification (scale bar = 20 µm). Similar results were also obtained in all other CNS tissues analyzed (data no shown).

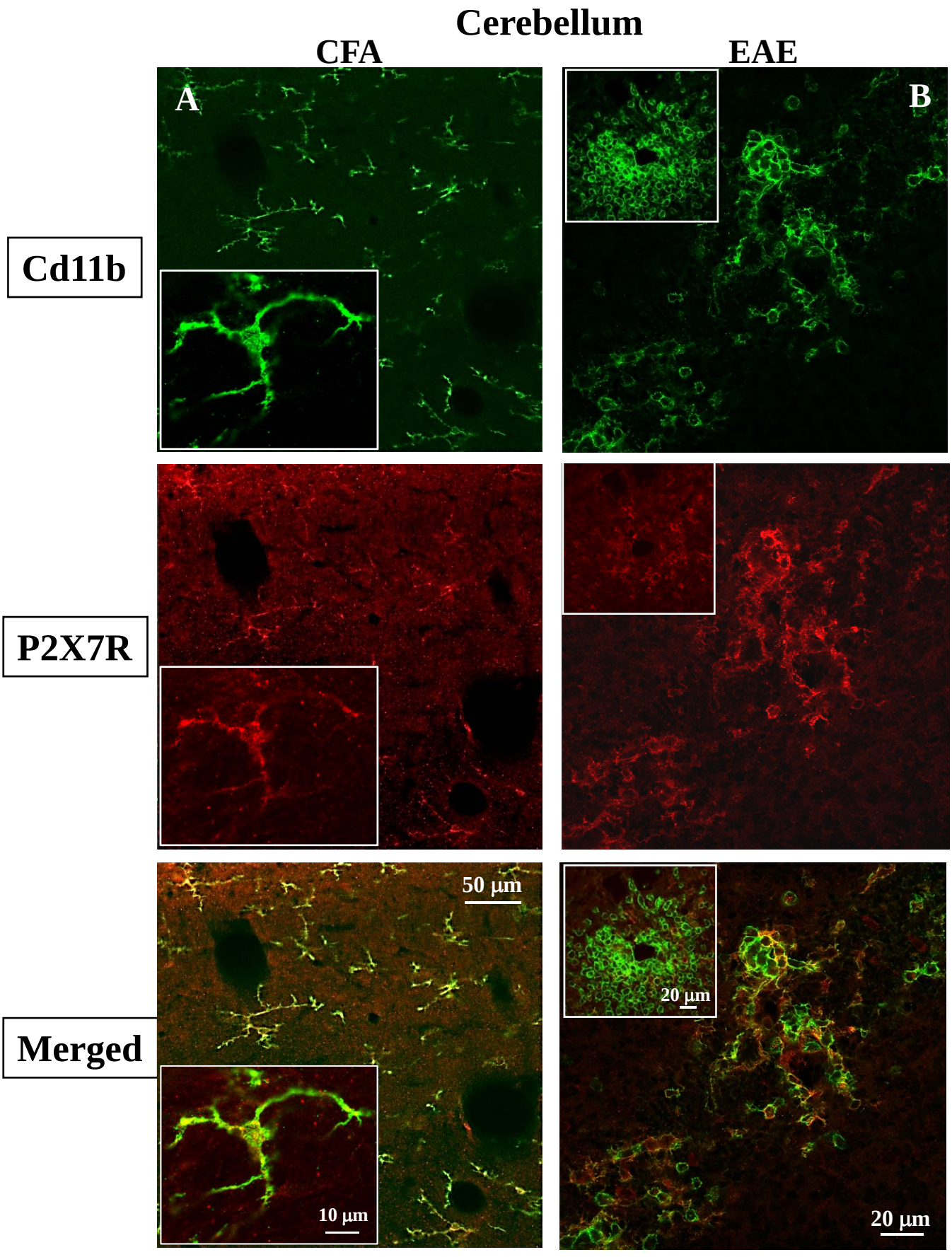
Cerebellum
CFA
EAE
A
B
Cd11b
P2X7R
Merged
50 μm
10 μm
20 μm
20 μm

Fig. 13. Presence of P2X7R on microglia cells. A, confocal analysis of double immunofluorescence shows that P2X7R (in red) colocalizes with Cd11b (in green) on ramified microglia in CFA tissue. Insets in A show microglial cell at higher magnification (scale bar = 10 μm). **B**, Microgliosis is increased in EAE tissue with respect to CFA. In cerebellum, P2X7R (in red) colocalizes with some Cd11b-positive microglia cells (in green), especially near blood vessels. These results are confirmed in all brain tissues analyzed (data no shown). Insets, in **B,** show a lower magnification of a blood vessel in cerebellum (scale bar = 20 μm). In the merged field in **A**, double immunofluorescent yellow signal is present in most microglia cells, while in the merged field in **B** double immunofluorescent yellow signal is present only in some cells.
Scale bars = 50 μm in **A**, 20 μm in **B**.

4.4 P2X7R mRNA and protein are present in peripheral blood mononuclear cells and MS cortical tissue extracts.

After having established the weak presence of P2X7R on microglia and lack of upregulation in acute EAE brain, we then investigated the presence and potential modulation of P2X7R in MS. Since microglia in the CNS derive from monocyte-macrophage cells present in the blood that enter the brain during embryonic, foetal and postnatal stages, or as a consequence of strong inflammation, we decided to analyse both PBMCs and CNS tissue for the presence of P2X7R. In particular, we studied MS cerebral cortex where neuron/axon injury is prominent and widespread in GM and the P2X7R is not characterized yet. Cryostat sections (30-40 μm thick) from PPMS and SPMS cerebral cortex were previously stained with Luxol fast blue and cresyl fast violet (Kluver-Barrera staining), in order to detect WM and GM lesions and their cellularity [152]. In WM, the lesions were characterized as active (with abundant amoeboid, round microglia) or inactive (with dense astrocytic scarring and ramified microglia), according to the morphological appearance of both major histocompatibility complex (MHC) II or GFAP-immunopositive cells.

We first performed RT-PCR on PBMCs and MS cortical extracts and demonstrated the presence of a single cDNA band of approximately 647 bp, exactly corresponding to the estimated amplicon length for P2X7R. A similar band was obtained also in MS samples (**Fig. 14A)**.

We then detected P2X7R protein by Western blot analysis in cortical extracts from 4 different cases of MS. Although within different expression levels, the receptor was recognized as a single specific protein band of about 75 kDa, which was abolished in the presence of the neutralizing P2X7R immunogenic peptide (**Fig. 14B**). Finally, by immunohistochemistry analysis, we proved the presence of P2X7R protein in MS cortical tissue and demonstrated that the P2X7R signal delineated the plasma membrane exclusively of cells located inside the lumen of blood vessels (**Fig. 14C**), being totally absent from the cortical parenchyma.

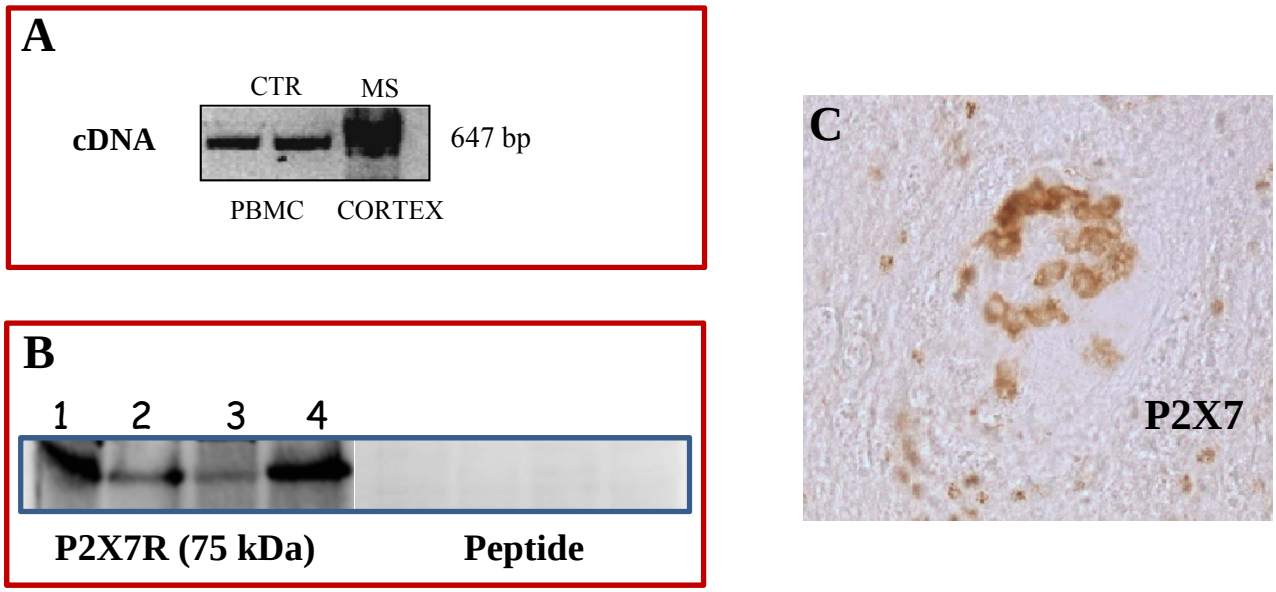

Fig. 14. P2X7R mRNA and protein are present in PMBC and MS cortical tissue. **A**, RT-PCR analysis shows that P2X7R mRNA is expressed on both control PBMC and MS cortex. A single cDNA band of approximately 647 bp is indicated. **B**, Western blot analysis of P2X7R protein confirms the presence of receptor in four different MS cerebral cortex extracts. Equal amount of total protein (30 μg/well) was separated by SDS-PAGE and transferred to nitrocellulose. Filters were stained with Ponceau-S and immunostained with rabbit anti-P2X7R serum, in the absence or presence of the neutralizing immunogenic peptide. Molecular mass of 75 kDa is indicated for the receptor. **C**, Immunohistochemistry staining was performed on MS frontal cortex using P2X7R antiserum. The receptor is present only in some cells inside a blood vessel.

4.5 P2X7R is not present on microglia, astrocytes and oligodendrocytes.

In order to define the cellular localization of P2X7R in MS cortex, we performed double-immunofluorescence confocal analysis on 13 total tissue blocks originating from 6 different MS cases with ages at death ranging from 34 to 80 years, stable or progressive activities of disease, disease durations spanning between 11 and 50 years and variable causes of death. We compared these results to two control cases that died not for neurological diseases. We found that MHCII clearly marked several ramified resting microglia (**Fig. 15A, a-b**, in green with Cy2 fluorescence), GFAP marked many fibrous astrocytes (**Fig. 15B, a-b**, in green with Cy2 fluorescence) and MBP identified longitudinal and transverse myelin fibers of various thickness and oligodendrocyte cell bodies (**Fig. 15C, a-b**, in green with Cy2 fluorescence) in MS cerebral cortex. In these same sections, specific P2X7R immunoreactivity was found always absent from microglia, astrocytes and oligodendrocytes in the tissue parenchyma. Positive P2X7R reactive signal was instead demonstrated only inside the blood vessels, in some cases adjacent to the blood vessel wall or even translocating through the wall (arrow head in **Fig. 15A** inset **a** and in **Fig. 15C**), and delineating the plasma membrane of few roundish cells (see arrows in **Fig. 15A-B-C**). These results were confirmed in all PPMS (MS129 and MS168) and SPMS (MS163, MS074 and MS079) cases analyzed.

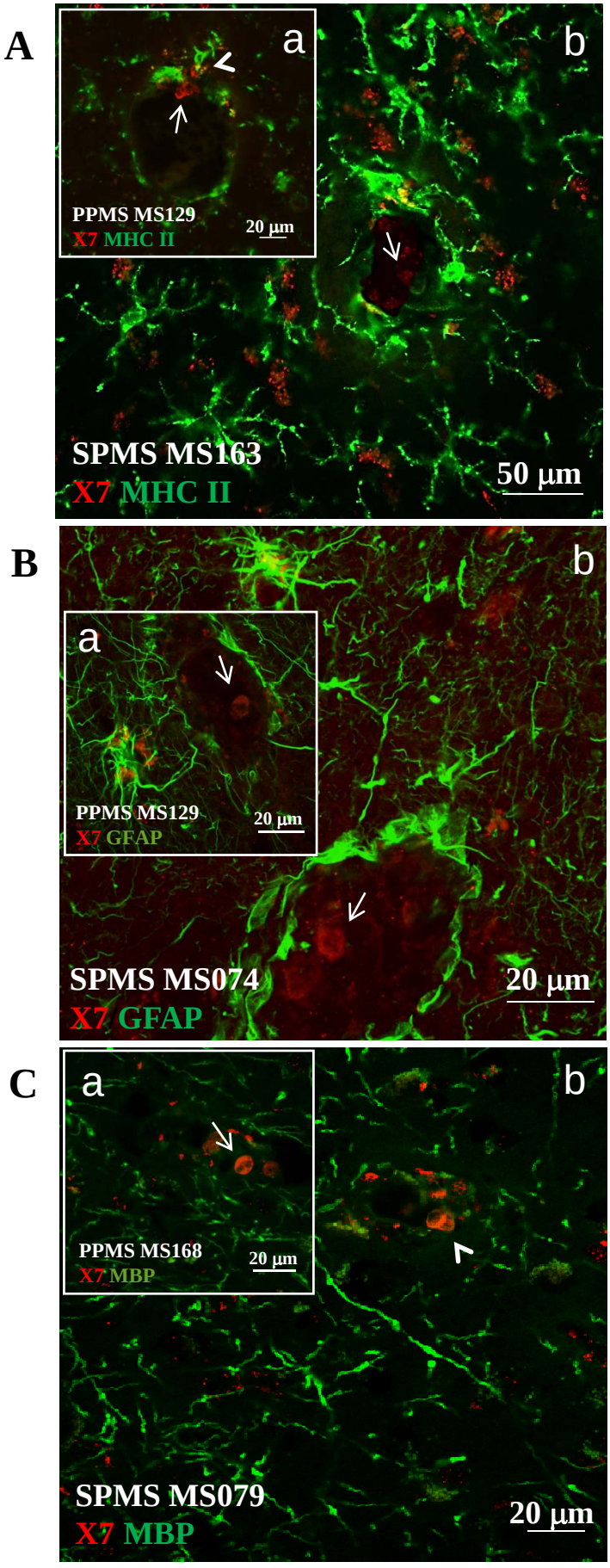

Fig. 15. Absence of P2X7R protein from microglia, astrocytes and oligodendrocytes in both PPMS and SPMS tissues.

Confocal images of double immunofluorescence were analyzed to investigate if the P2X7R (in red, Cy3 fluorescence) is present on microglia (**A**), astrocytes (**B**), and oligodendrocytes (**C**) (all in green, Cy2 fluorescence) in PPMS (d) and SPMS tissue (e). P2X7R immunoreactive cells in **A**, **B**, and **C** pertain neither to MHC II-immunoreactive microglia (**A**), nor to GFAP-positive astrocytes (**B**), nor to MBP-positive oligodendrocytes (**C**), in both PPMS and SPMS tissues.

Positive cells for P2X7R are found only inside (red, arrows) or adjacent blood vessels(red, arrow head) . Scale bars = 20 µm in A(a), B(a), C(a), B(b), C(b) and 50 µm in A(b).

4.6 P2X7R signal is present in MS cortical blood vessels.

At this point, we performed double immunofluorescence confocal analysis in order to identify the specific immunopositive cell phenotypes expressing P2X7R inside the blood vessel. We used CD45 (labelling all hematopoietic cells with the exception of erythrocytes and platelets) and CD14 (staining monocytes) as markers. We demonstrated strong co-localization between P2X7R and CD45 inside the blood vessels, although not all CD-45 positive cells simultaneously co-express P2X7R (**Fig. 16A**). Conversely, all CD14-positive cells located in the blood lumen were simultaneously recognized by the P2X7R antiserum (**Fig. 16B**). The P2X7R immunoreactive signal was instead apparently absent from CD14-positive endothelial cells of the blood vessels that are also positive for CD68/MHC II (macrophages/microglia marker) (see arrows in **Fig. 17A and B**). This further confirms the absence of P2X7R from microglia/macrophages that we found also in the parenchyma of MS cortex.

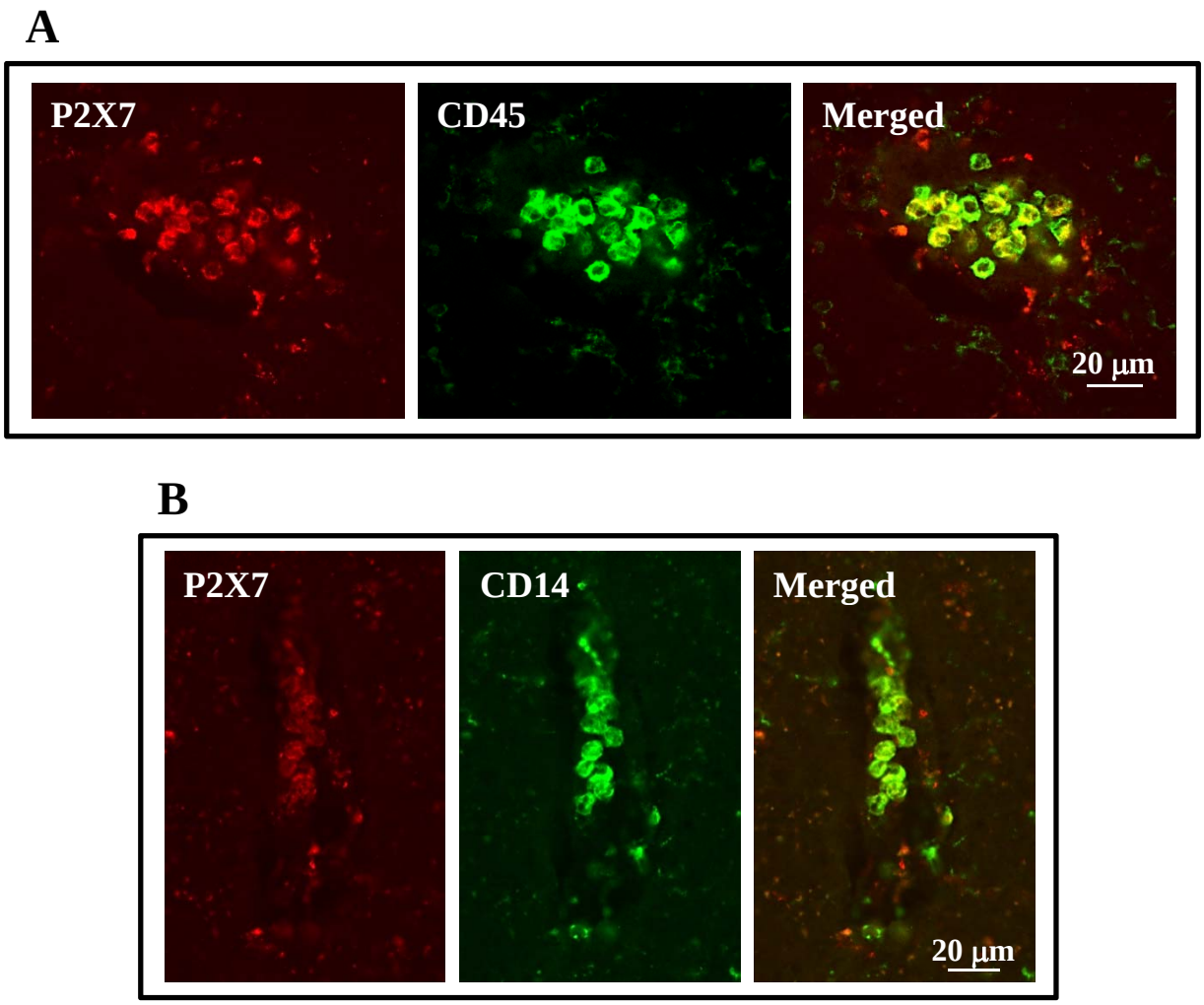

Fig. 16. Presence of P2X7R in MS cortical monocytes. Double immunofluorescence was performed in order to characterize P2X7R positive cells in MS cortical blood vessels. **A**, Confocal images show colocalization between P2X7R (red) and CD45 in almost all leukocytes (green) present inside a blood vessel. **B**, Double immunofluorescence with P2X7R (red) and CD14 (green) demonstrates that the leukocytes positive for P2X7R are CD14-positive monocytes. Scale bars = 20 μm in **A** and **B**.

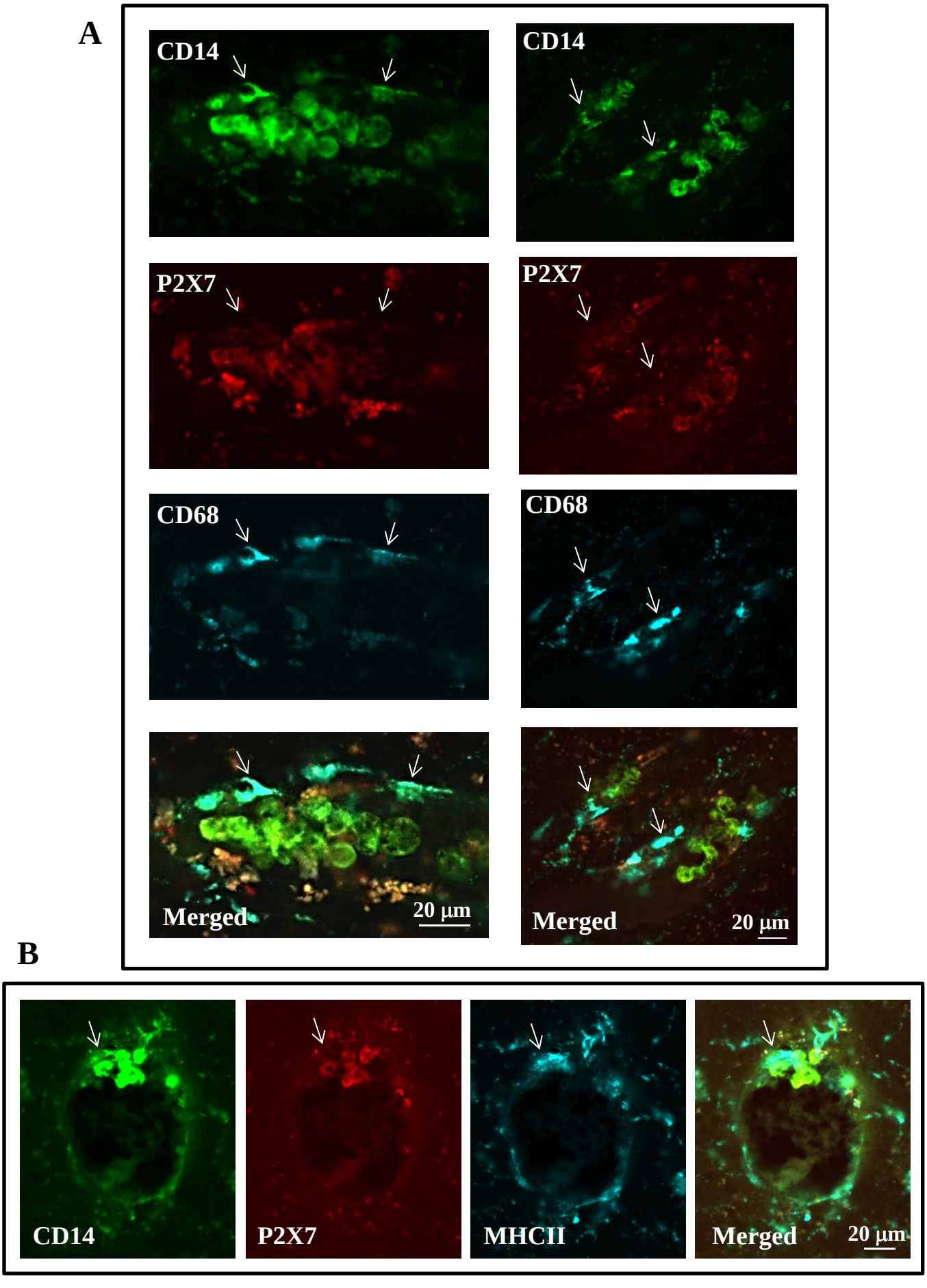
A
CD14
CD14
P2X7
P2X7
CD68
CD68
Merged
20 µm
Merged
20 µm
B
CD14
P2X7
MHCII
Merged
20 µm

Fig. 17. Absence of P2X7R in blood vessel endothelium. Triple immunofluorescence visualized by confocal analysis with different immunoreactive markers was performed on sections from MS frontal cortex. **A**, **B** CD14 (monocytes, green, Cy2 immunofluorescence), P2X7R (red, Cy3 immunofluorescence), and CD68/MHC II (microglia/macrophages, blue, Cy5 immunofluorescence). In the lumen of blood vessels, the P2X7R colocalizes with CD14, while the receptor is absent from microglia/macrophages present in the blood vessel endothelium (see arrows in **A** and **B**). In the merged field, the absence of triple immunofluorescent white signal indicates absence of cells simultaneously positive for CD14, P2X7R, and CD68/MHC II. Yellow signal indicates cells lacking Cd68/MHC II, but positive for CD14 and P2X7R. Light blue signal indicates cells lacking P2X7R, but positive for CD14 and CD68/MHC II. Scale bars = 20 μm in **A** and **B**.

4.7 Modulation of P2X7 receptor expression in monocytes upon LPS and BzATP stimuli.

Having established from the above results that parenchimal MS cortical tissue apparently lacks of P2X7R immunoreactivity, and the receptor is instead highly expressed in mononuclear blood cells, we verified if the receptor is modulated in MS blood cells and in particular on monocytes.

We performed FACS analysis on freshly isolated PBMCs from MS patients in different phases of disease activity and we confirmed that MS monocytes express P2X7R. In particular, the receptor resulted significantly downregulated in CD14-positve cells of MS acute compared to MS stable patients (*$p<0.05$) (**Fig. 18**).

Moreover, we stimulated monocytes from healthy donors with pro-inflammatory stimuli 100 ng/ml LPS or 250 μM BzATP for 4 and 24 hours, to analyze P2X7R expression *in vitro*. Afetr both treatments, we observed a downregulation of P2X7R during the time course. In particular the receptor expression decreased of about 40% at 4 hours and about 70% at 24 hours after LPS stimulation compared to no treatment (**Fig. 19A**). We confirmed this trend also after BzATP stimulation, and found that P2X7R expression decreased of about 7% at 4 hours and about 50% at 24 hours compared to control (**Fig. 19B**).

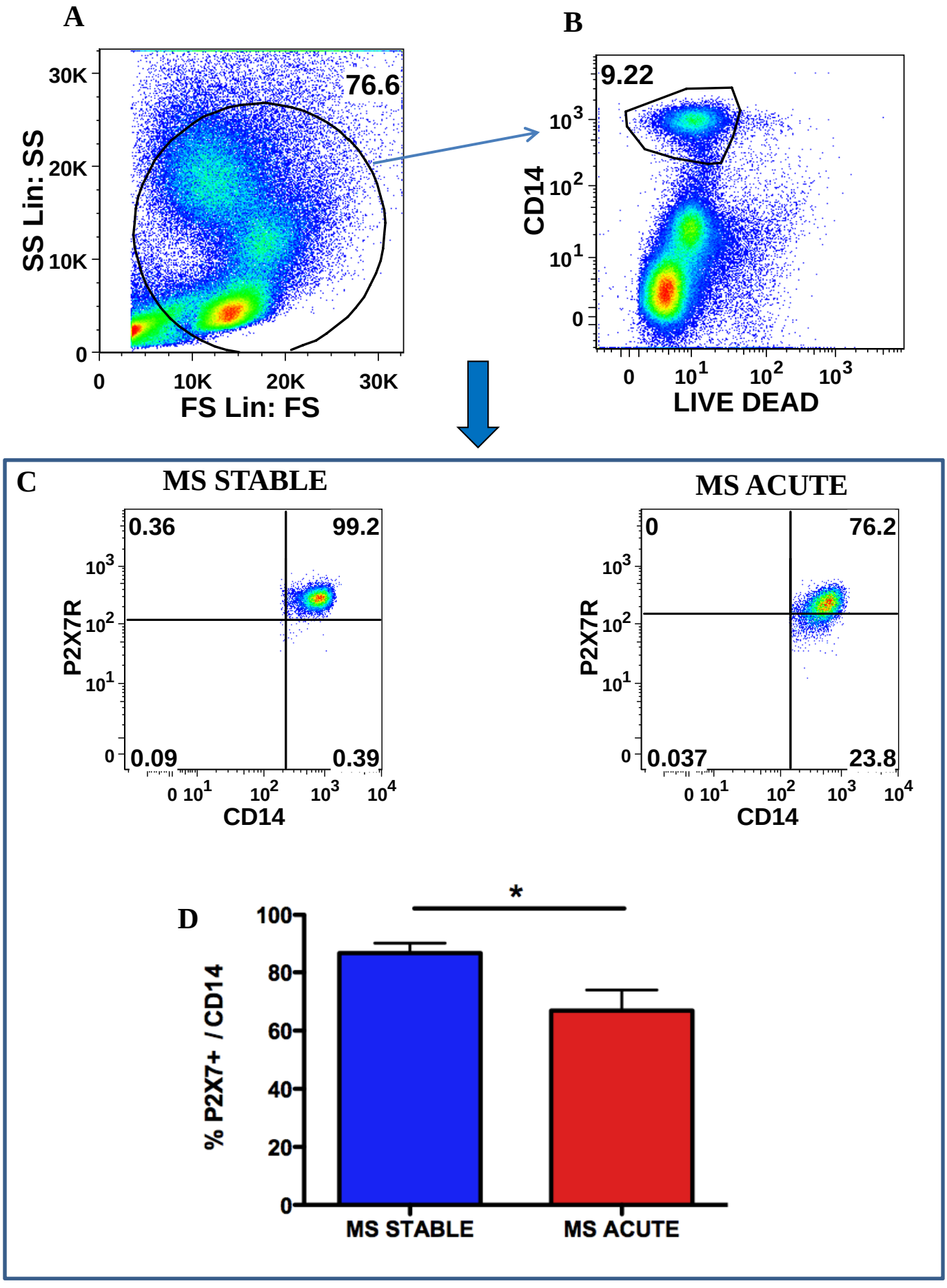
A
B
76.6
SS Lin: SS
FS Lin: FS
9.22
CD14
LIVE DEAD
C
MS STABLE
MS ACUTE
0.36
99.2
0.09
0.39
0
76.2
0.037
23.8
P2X7R
CD14
D
*
% P2X7+ / CD14
MS STABLE
MS ACUTE

Fig 18. P2X7R expression in PBMC by FACS analysis. A, characteristic forward (FS, x-axis) and side (SS, y-axis) scatter profiles of PBMC. In **B,** monocytes were characterized as CD14+ cells. Live Dead was used to discriminate viable cells.
C, P2X7R expression was analyzed within CD14-positive cells and we show representative plots of MS patients in stable and acute phases. In **D**, we show cumulative data from 10 stable MS and 4 acute MS patients.

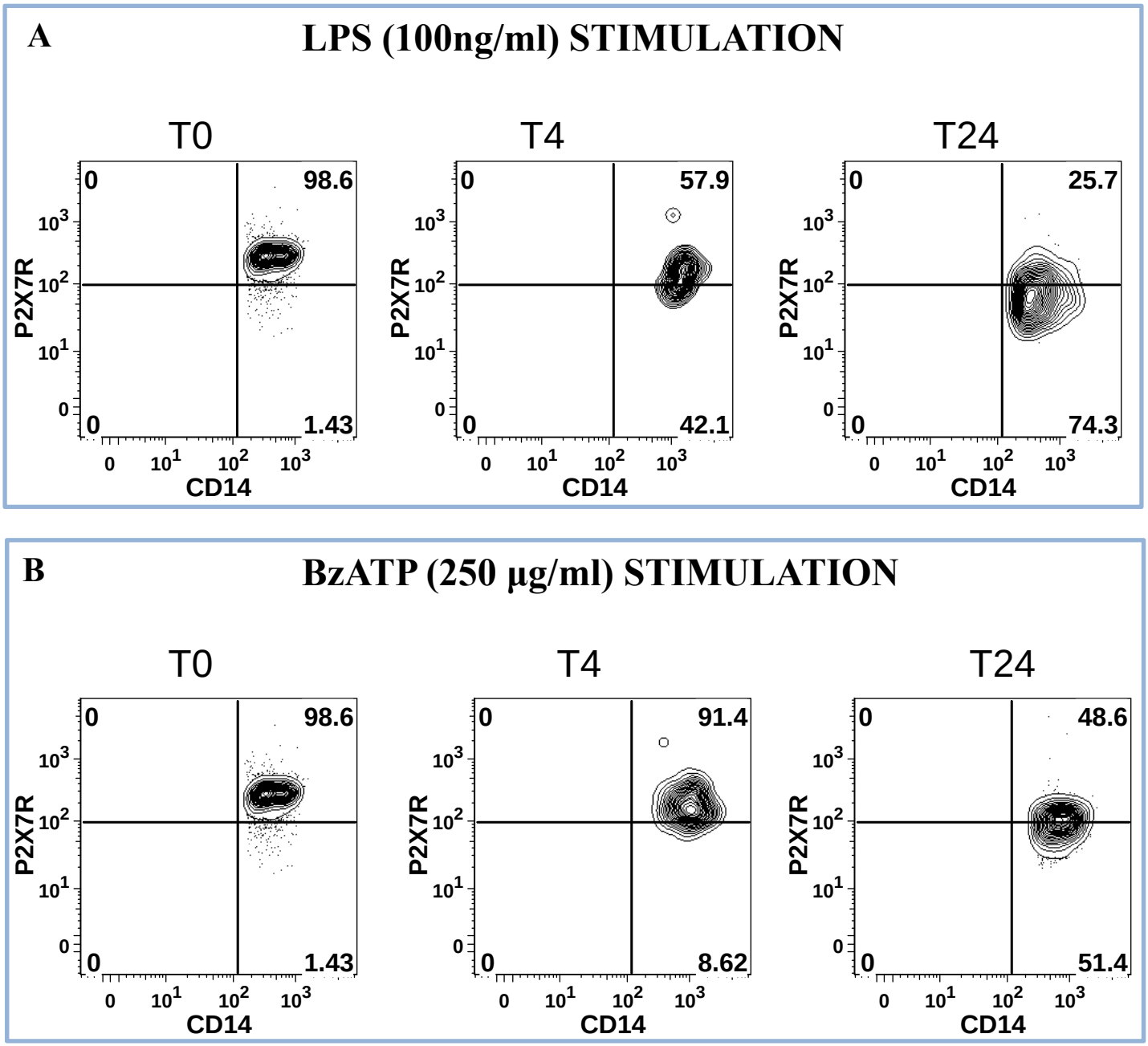

Fig. 19 P2X7R downregulation after LPS and BzATP stimuli.

A , Representative plot of modulation of P2X7R after LPS stimulation (T0: no treatment, T4: treatment for 4 hours, T24: treatment for 24 hours).

B, Representative plot of modulation of P2X7R after BzATP stimulation (T0: no treatment, T4: treatment for 4 hours, T24: treatment for 24 hours).

LPS and BzATP both down regulate the P2X7R expression on monocytes from healthy subjects.

Discussion

The aim of this thesis was to examine the P2X7R involvement in MS pathogenesis, by employing both the EAE rat model for MS, as well as PBMCs and CNS autoptic tissue from MS patients.

EAE is one of the most commonly used experimental model for the human inflammatory demyelinating disease, MS. EAE is a complex condition in which the interaction between a variety of immunopathological and neuropathological mechanisms leads to an approximation of key pathological features of MS: inflammation, demyelination, gliosis and axonal loss. The counter-regulatory mechanisms of resolution of inflammation and remyelination also occur in EAE, which therefore can also serve as a model for these processes. Moreover, EAE is often used as a model of cell-mediated organ-specific autoimmune conditions in general. EAE has a complex neuropharmacology, and many of the drugs that are in current or imminent use in MS have been developed, tested or validated on the basis of EAE studies. However, there is great heterogeneity in the susceptibility to the induction, the method of induction and the response to various immunological or neuropharmacological interventions. This makes EAE a very versatile system to use in translational neuro- and immunopharmacology, but the model needs to be tailored to the scientific question being asked. While creating difficulties and underscoring the inherent weaknesses of this model of MS in straightforward translation from EAE to the human disease, this variability also creates an opportunity to explore the multiple facets of the immune and neural mechanisms of immune-mediated neuroinflammation and demyelination as well as intrinsic protective mechanisms [163].

Although a role of T cells, particularly in their ability to initiate disease in EAE and MS, has been well documented [164], other cell types including astrocytes, microglia, and macrophages are also critical for the evolution and maintenance of neuroinflammation via mechanisms such as reactivation of T cells, production of proinflammatory cytokines, and phagocytosis of myelin [165]. For instance, macrophage/microglia migration and activation in the CNS are critical for the demyelination and clinical signs of EAE. Therefore, in this thesis, in order to assess the frequency

of macrophages/microglia as well as astrocytes in the CNS of rat injected with CFA or with the immunogenic EAE mixture, serial brain sections were stained with CD11b, a marker for microglia/macrophages, and GFAP, a marker for astrocytes, and analyzed by immunohistochemistry and immunofluorescence confocal analysis. As previously described [163,166], we confirmed intense gliosis in cortex, corpus callosum, striatum, septum and cerebellum, more pronounced in EAE with respect to CFA rats. In particular, we observed more abundant and fibrous astrocytes occupying all the EAE brain parenchyma, together with an increased number of ramified microglia in the same areas. Increased microgliosis and presence of duplicating/phagocytic microglia was found very abundant especially in proximity to blood vessels in EAE, but not in CFA cerebellum. Indeed, a spatiotemporal analysis of the pathogenesis of EAE has previously indicated that periventricular and superficial white matter structures are primary targets of early T-cell infiltration [167]. This might be reason why we noticed more infiltrated microglia cells exclusively around blood vessels in cerebellum and septum. Since P2X7R was weakly expressed only on ramified resting microglia but not on astrocytes in CFA brain parenchyma, and it was moreover more abundantly expressed on roundish (phagocytic/duplicating) microglia in the surroundings of EAE blood vessels, we might hypothesise that either extravasation and infiltration of immune competent cells into the CNS parenchyma from the blood stream, or recruitment of microglia/macrophages from the parenchyma towards the blood vessels where the neurotoxic agents are more abundantly present, might occur in concomitance with P2X7R expression in EAE. Further studies will help to explain which condition is indeed occurring between these two, and the underlying molecular mechanisms.

A critical step in the development of brain inflammation is in fact the adhesion of leukocytes on endothelial cells and their subsequent migration through the BBB into the CNS tissue. Microglia and blood-derived myelomonocytes have both been implicated in the development of EAE and MS because of their ability to present antigens, secrete pro-inflammatory cytokines and participate in demyelination by phagocytosis of degraded myelin. However, it is unclear whether these two cell

types have distinct roles in MS pathogenesis [168]. Because the P2X7R has an ubiquitous distribution in nearly all tissues and organs of the body with the highest expression in immune cells of monocytes-macrophage origin [169], and activation of P2X7R in lymphoid leukocytes triggers multiple responses that shape the intensity and duration of innate immune and inflammatory responses [170], we investigated the presence of the receptor in both peripheral blood mononuclear cells, as well as CNS autoptic tissue from PPMS and SPMS patients. Using different approaches, mainly RT-PCR, Western blotting, immunohistochemistry and immunofluorescence confocal analysis, we confirmed the presence of P2X7R in MS CNS tissue, thus corroborating previous results establishing for instance the expression of the receptor in MS optic nerve [154], spinal cord [67]. However, our results of PPMS and SPMS cortical tissue didn't confirm the expression of P2X7R at the cellular level on astrocytes [171], olygodendrocytes [154] and microglia [67]. These discrepancies might be due to tissue specificity of P2X7R expression, to PPMS/SPMS versus acute phases of MS, to human sampling variability. Moreover, also differently from the EAE tissue that we described above, P2X7R was neither present on resting or activated microglia in MS cerebral cortex, but the receptor was instead demonstrated in PPMS and SPMS brain exclusively on monocytes (CD45/CD14 positive) found in the lumen of blood vessels in cortical areas characterized by high levels of inflammation and cell infiltration. Remarkably, this same distribution was not demonstrated on CNS tissue from healthy donors, where the blood vessels present in cerebral cortex were totally devoid of leukocyte/monocyte infiltrates. The presence of P2X7R on monocytes in MS brain thus validates recent reports on the localization of the receptor on monocytes in peripheral blood from MS patients [157]. However, receptor expression seemed perhaps to disappear during the differentiation of monocytes to macrophages, thus suggesting that monocyte activation might interfere with P2X7R expression.

In conclusion, the first finding of this work is the recognition of a widespread specie-specific difference in the expression of P2X7R in rat (present only in microglia in EAE brain tissue) and human (present only in monocytes in MS cortex), in concomitance with the insurgence of severe

diseases characterized by increased numbers of lymphocytes and activated macrophage/microglia penetrating the CNS parenchyma from the peripheral blood stream, that are MS and EAE, the animal model for MS. However, such differences might be additionally ascribed to the respective acute or progressive phases of the disease characterizing EAE or PPMS/SPMS. Further studies will alternatively discern if the EAE animal model is instead not completely exhaustive for understanding the course of MS. On this matter, previous studies have indeed established that acute EAE in rat is a reliable animal model to study especially the principal mechanisms involved in T cell-mediated CNS inflammation, rather than a multifaceted pathology such as MS [172].

The second major result that we presented in this thesis is that P2X7R expression appears to decrease after activation of monocytes/macrophages occurring during their extravasation from the blood stream to the CNS parenchyma in MS. This might imply that while activation of P2X7R is carrier of an inflammatory signal in the periphery, its down regulation in the CNS tissue represents a beneficial attempt to reduce damage and inflammation. This is consistent with the reduction of P2X7R expression found in CD14-positive monocytes in acute with respect to stable MS patients. This hypothesis was furthermore confirmed with purified CD14-posivite monocytes from healthy donors that demonstrated a marked reduction of P2X7R expression when placed *in vitro* and activated by bacterial LPS or BzATP, both inducing activation and insurgence of a more inflammatory phenotype [157,173].

In other words, while leaving some questions still unsettled and providing novel evidence for P2X7R involvement in EAE and MS, the present thesis will surely stimulate useful discussion on the topic.

Bibliografy

1. Ralevic V, Burnstock G. Receptors for purines and pyrimidines. *Pharmacol Rev*, 1998, 50(3): 413-92.

2. North RA, Barnard EA. Nucleotide receptors. *Curr Opin Neurobiol*, 1997, 7(3): 346-57.

3. Burnstock G. Physiology and Pathophysiology of Purinergic Neurotransmission. *Physiol Rev*, 2007, 87: 659–797.

4. Zimmermann H. Ectonucleotidases: some developments and a note on nomenclature. *Drug Dev Res*, 2001, 52: 44-56.

5. Robson S, Sévigny J, Zimmermann H. The E-NTPDase family of ectonucleotidases: structure function relationships and pathophysiological significance. *Purinergic Signal*, 2006, 2: 409-30.

6. Bonan CD, Schetinger MRC, Battastini AMO, Sarkis JJF. Ectonucleotidases and synaptic plasticity: implications in physiological and pathological conditions. *Drug Dev Res*, 2001, 52: 57-65.

7. Rassendren F, Buell GN, Virginio C, Collo G, North RA, Surprenant A. The permeabilizing ATP receptor, P2X7. Cloning and expression of a human cDNA. *J Biol Chem*, 1997, 272(9): 5482-5486.

8. Buell GN, Talabot F, Gos A, Lorenz J, Lai E, Morris MA, Antonarakis SE. Gene structure and chromosomal localization of the human P2X7 receptor. *Recept Chann*, 1998, 5(6): 347-354.

9. Cheewatrakoolpong B, Gilchrest H, Anthes JC, Greenfeder S. Identification and characterization of splice variants of the human P2X7 ATP channel. *Biochem Biophys Res Commun*, 2005, 332: 17–27.

10. Feng YH, Li X, Wang L, Zhou L, Gorodeski GI. A truncated P2X7 receptor variant (P2X7-j) endogenously expressed in cervical cancer cells antagonizes the full-length P2X7 receptor through hetero-oligomerization. *J Biol Chem*, 2006, 281: 17228–37.

11. Hansen MA, Barden JA, Balca VJ, Keay KA, Bennett MR. Structural motif and characteristics of the extracellular domain of P2X receptors. *BBRC*, 1997, 236: 670-675.

12. Amstrup J, Novak I. P2X7 receptor activates extracellular signal-regulated kinases ERK1 and ERK2 independently of Ca2+ influx. *Biochem J*, 2003, 374 (Pt 1), 51-61.

13. Teixeira PC, de Souza CA, de Freitas MS, Foguel D, Caffarena ER, Alves LA. Predictions suggesting a participation of beta-sheet configuration in the M2 domain of the P2X(7) receptor: a novel conformation? *Biophys J*, 2009, 96(3): 951-963.

14. Costa-Junior HM, Sarmento Vieira F, Coutinho-Silva R. C terminus of the P2X7 receptor: treasure hunting. *Purinergic Signal*, 2011, 7(1): 7-19.

15. Kim M, Spelta V, Sim J, North RA, Surprenant A. Differential assembly of rat purinergic P2X7 receptor in immune cells of the brain and periphery. *J Biol Chem*, 2001, 276(26): 23262-23267.

16. Casas-Pruneda G, Reyes JP, Pérez-Flores G, Pérez-Cornejo P, Arreola J. Functional interactions between P2X4 and P2X7 receptors from mouse salivary epithelia. *J Physiol*, 2009, 587(Pt 12): 2887-2901.

17. Nicke A. Homotrimeric complexes are the dominant assembly state of native P2X7 subunits. *Biochem Biophys Res Comm*, 2008, 377: 803-808.

18. Kim M, Jiang LH, Wilson HL, North RA, Surprenant A. Proteomic and functional evidence for a P2X7 receptor signalling complex. *EMBO J*, 2001, 20: 6347-6358.

19. Wilson HL, Wilson SA, Surprenant A, North RA. Epithelial membrane proteins induce membrane blebbing and interact with the P2X7 receptor C terminus. *J Biol Chem*, 2002, 277: 34017-34023.

20. Guo C, Masin M, Qureshi OS, Murrell-Lagnado RD. Evidence for functional P2X4/P2X7 heteromeric receptors. *Mol Pharmacol*, 2007, 72(6): 1447-1456.

21. Volonté C, Apolloni S, Skaper SD and Burnstock G. P2X7 Receptors: Channels, Pores and More. *CNS Neurol Disord Drug Targets*, 2012, 11(6): 705-21.

22. North R.A. Molecular physiology of P2X receptors. *Physiol Rev*, 2002, 82: 1013-1067.

23. Rassendren F, Buell G, Newbolt A, North RA, Surprenant A. Identification of amino acid residues contributing to the pore of a P2X receptor. *EMBO J* 1997, 16: 3446-3454.

24. Pelegrin P, Surprenant A. The P2X(7) receptor-pannexin connection to dye uptake and IL-1beta release. *Purinergic Signal*, 2009, 5: 129-137.

25. Teixeira PC, de Souza CA, de Freitas MS, Foguel D, Caffarena ER, Alves LA. Predictions suggesting a participation of beta-sheet configuration in the M2 domain of the P2X(7) receptor: a novel conformation? *Biophys J*, 2009, 96(3): 951-963.

26. Donnelly-Roberts DL, Namovic MT, Faltynek CR, Jarvis MF. Mitogen-activated protein kinase and caspase signaling pathways are required for P2X7 receptor(P2X7R)-induced pore formation in human THP-1 cells. *J Pharmacol Exp Ther*, 2004, 308(3): 1053-1061.

27. Donnelly-Roberts DL, Namovic MT, Han P, Jarvis MF. Mammalian P2X7 receptor pharmacology: comparison of recombinant mouse, rat and human P2X7 receptors. *Br J Pharmacol*, 2009, *157*(7): 1203-1214.

28. Donnelly-Roberts DL, Jarvis MF. Discovery of P2X7 receptorselective antagonists offers new insights into P2X7 receptor function and indicates a role in chronic pain states. *Br J Pharmacol*, 2007, 151(5): 571-579.

29. Marques-da-Silva C, Chaves MM, Castro NG, Coutinho-Silva R, Guimaraes MZP. Colchicine inhibits cationic dye uptake induced by ATP in P2X2- and P2X7-expressing cells: implication for its therapeutic action. *Br J Pharmacol*, 2011, 163: 912-926.

30. Iglesias R, Locovei S, Roque A, Alberto AP, Dahl G, Spray DC, Scemes E. P2X7 receptor-Pannexin1 complex: pharmacology and signaling. *Am J Physiol Cell Physiol*, 2008, 295(3): C752-C760.

31. Pelegrin P, Surprenant A. Pannexin-1 mediates large pore formation and interleukin-1beta release by the ATP-gated P2X7 receptor. *EMBO J*, 2006, 25(21): 5071-5082.

32. Hanley PJ, Kronlage M, Kirschning C, Del Rey A, Di Virgilio F, Leipziger J, Chessell IP, Sargin S, Filippov MA, Lindemann O, Mohr S, Koenigs V, Schillers H, Baehle M, Schwab A. Transient P2X7 receptor activation triggers macrophage death independent of TLR2/*4*, Casp1 and Panx1. *J Biol Chem*, 2012, 287(13): 10650-10663.

33. Coddou C, Yan Z, Obsil T, Huidobro-Toro JP, Stojilkovic SS. Activation and regulation of purinergic P2X receptor channels. *Pharmacol Rev*, 2011, 63(3): 641-83.

34. Yan Z, Khadra A, Li S, Tomic M, Sherman A, Stojilkovic SS. Experimental characterization and mathematical modeling of P2X7 receptor channel gating. *J Neurosci*, 2010, 30(42): 14213-14224.

35. Roger S, Gillet L, Baroja-Mazo A, Surprenant A, Pelegrin P. C-terminal calmodulin-binding motif differentially controls human and rat P2X7 receptor current facilitation. *J Biol Chem*, 2010, 285: 17514-17524.

36. Franke H, Verkhratsky A, Burnstock G, Illes P. Pathophysiology of astroglial purinergic signalling. *Purinergic Signal*, 2012, 8(3): 629-57.

37. Collo G, Neidhart S, Kawashima E, Kosco-Vilbois M, North RA, Buell G. Tissue distribution of the P2X7 receptor. *Neuropharmacology*, 1997, 36: 1277-1283.

38. Cavaliere F, Dinkel K, Reymann K. Microglia response and P2 receptor participation in oxygen/glucose deprivation-induced cortical damage. *Neuroscience*, 2005, 136: 615-623.

39. Melani A, Amadio S, Gianfriddo M, Vannucchi MG, Volonté C, Bernardi G, Pedata F, Sancesario G. P2X7 receptor modulation on microglial cells and reduction of brain infarct caused by middle cerebral artery occlusion in rat. *J Cereb Blood Flow Metab*, 2006, 26: 974-982.

40. Ballerini P, Rathbone MP, Di Iorio P, Renzetti A, Giuliani P, D'Alimonte I, Trubiani O, Caciagli F, Ciccarelli R. Rat astroglial P2Z (P2X7) receptors regulate intracellular calcium and purine release. *NeuroReport*, 1996, 7: 2533-2537.

41. Wirkner K, Kofalvi A, Fischer W, Gunther A, Franke H, Groger-Arndt H, Norenberg W, Madarasz E, Vizi ES, Schneider D, Sperlágh B, Illes P. Supersensitivity of P2X7 receptors in cerebrocortical cell cultures after in vitro ischemia. *J Neurochem*, 2005, 95: 1421-1437.

42. James G, Butt AM. P2Y and P2X purinoceptor mediated Ca2+ signalling in glial cell pathology in the central nervous system. *Eur J Pharmacol*, 2002, 447: 247-260.

43. Amadio S, D'Ambrosi N, Cavaliere F, Murra B, Sancesario G, Bernardi G, Burnstock G, Volonté C. P2 receptor modulation and cytotoxic function in cultured CNS neurons. *Neuropharmacology*, 2002, 42: 489-501.

44. Wang X, Arcuino G, Takano T, Lin J, Peng WG, Wan P, Li P, Xu Q, Liu QS, Goldman SA, Nedergaard M. P2X7 receptor inhibition improves recovery after spinal cord injury. *Nat Med*, 2004, 10: 821-827.

45. Sperlágh B, Kofalvi A, Deuchars J, Atkinson L, Milligan CJ, Buckley NJ, Vizi ES. Involvement of P2X7 receptors in the regulation of neurotransmitter release in the rat hippocampus. *J Neurochem*, 2002, 81: 1196-1211.

46. Deuchars SA, Atkinson L, Brooke RE, Musa H, Milligan CJ, Batten TF, Buckley NJ, Parson SH, Deuchars J. Neuronal P2X7 receptors are targeted to presynaptic terminals in the central and peripheral nervous system. *J Neurosci*, 2001, 21: 7143-7152.

47. Anderson CM, Nedergaard M. Emerging challenges of assigning P2X7 receptor function and immunoreactivity in neurons. *Trends Neurosci*, 2006, 29: 257-262.

48. Yu Y, Ugawa S, Ueda T, Ishida Y, Inoue K, Nyunt AK, Umemura A, Mase M, Yamada K, Schimada S. Cellular localization of P2X7 receptor mRNA in the rat brain. *Brain Research*, 2008, 1194: 45-55.

49. Ferrari D, Chiozzi P, Falzoni S, Hanau S, Di Virgilio F. Purinergic modulation of interleukin-1β release from microglial cells stimulated with bacterial endotoxin. *J Exp Med*, 1997, 185: 579–582.

50. Chakfe Y, Seguin R, Antel J P, Morissette C, Malo D, Henderson D, Séguéla P. ADP and AMP induce interleukin-1β release from microglial cells through activation of ATP-primed P2X7 receptor channels. *J Neurosci*, 2002, 22: 3061–3069.

51. Filippini A, Taffs RE, Agui T, Sitkovsky MV. Ecto-ATPase activity in cytolytic T-lymphocytes. Protection from the cytolytic effects of extracellular ATP. *J Biol Chem*, 1990, 265: 334–340.

52. Sikora A, Liu J, Brosnan C, Buell G, Chessel I, Bloom BR. Cutting edge: purinergic signaling regulates radical-mediated bacterial killing mechanisms in macrophages through a P2X7-independent mechanism. *J Immunol*, 1999, 163: 558–561.

53. Ferrari D, Chiozzi P, Falzoni S, Dal Susino M, Collo G, Buell G, Di Virgilio F. ATP-mediated cytotoxicity in microglial cells. *Neuropharmacology*, 1997, 36: 1295–1301.

54. Beigi R, Kobatake E, Aizawa M, Dubyak GR. Detection of local ATP release from activated platelets using cell surface-attached firefly luciferase. *Am J Physiol Cell Physiol*, 1999, 276: 267–278.

55. Dubyak GR, el-Moatassim C. Signal transduction via P2-purinergic receptors for extracellular ATP and other nucleotides. *Am J Physiol Cell Physiol*, 1993, 265: 577–606.

56. Lazarowski ER, Boucher RC, Harden TK. Constitutive release of ATP and evidence for major contribution of ecto-nucleotide pyrophosphatase and nucleosidediphosphokinase to extracellular nucleotide concentrations. *J Biol Chem*, 2000, 275: 31061–31068.

57. Nieber K, Eschke D, Brand E. Brain hypoxia: effects of ATP and adenosine. *Prog Brain Res*, 1999, 120: 287–297.

58. Skaper SD, Debetto P, Giusti P. The P2X7 purinergic receptor: from physiology to neurological disorders. *Faseb J*, 2010, 24(2): 337-45.

59. Monif M, Reid CA, Powell KL, Smart ML, Williams DA. The P2X7 receptor drives microglial activation and proliferation: a trophic role for P2X7R pore. *J Neurosci*, 2009, 29(12): 3781-91.

60. Garden GA. Microglia in human immunodeficiency virus-associated neurodegeneration. *Glia*, 2002, 40: 240–51.

61. Tan J, Town T, Paris D, Placzek A, Parker T, Crawford F, Yu H, Humphrey J, Mullan M. Activation of microglial cells by the CD40 pathway: relevance to multiple sclerosis. *J Neuroimmunol*, 1999, 97: 77–85.

62. Boje KM, Arora PK. Microglial-produced nitric oxide and reactive nitrogen oxides mediate neuronal cell death. *Brain Res*, 1992, 587: 250–256.

63. Kim YS, Joh TH. Microglia, major player in the brain inflammation: their roles in the pathogenesis of Parkinson's disease. *Exp Mol Med*, 2006, 38: 333-347.

64. Danton GH, Dietrich WD. Inflammatory mechanisms after ischemia and stroke. *J Neuropathol Exp Neurol*, 2003, 62: 127-136.

65. Suzuki T, Hide I, Ido K, Kohsaka S, Inoue K, Nakata Y. Production and release of neuroprotective tumor necrosis factor by P2X7 receptor-activated microglia. *J Neurosci*, 2004, 24: 1-7.

66. Monif M, Burnstock G, Williams DA. Microglia: Proliferation and activation driven by the P2X7 receptor. *Int J Biochem Cell Biol*, 2010, 42(11): 1753-6.

67. Yiangou Y, Facer P, Durrenberger P, Chessell IP, Naylor A, Bountra C, Banati RR, Anand P. COX-2, CB2 and P2X7-immunoreactivities are increased in activated microglial cells/macrophages of multiple sclerosis and amyotrophic lateral sclerosis spinal cord. *BMC Neurol*, 2006, 6: 12.

68. Diaz-Hernandez M, Diez-Zaera M, Sanchez-Nogueiro J, Gomez-Villafuertes R, Canals JM, Alberch J, Miras-Portugal MT, Lucas JJ. Altered P2X7-receptor level and function in mouse models of Huntington's disease and therapeutic efficacy of antagonist administration. *FASEB J*, 2009, 23: 1893-1906.

69. Le Stunff H, Raymond MN. P2X7 receptor-mediated phosphatidic acid production delays ATP-induced pore opening and cytolysis of RAW 264.7 macrophages. *Cell Signal*, 2007, 19: 1909-1918.

70. Bringmann A, Pannicke T, Moll V, Milenkovic I, Faude F, Enzmann V, Wolf S, Reichenbach A. Upregulation of P2X(7) receptor currents in Muller glial cells during proliferative vitreoretinopathy. *Invest Ophtalmol Vis Sci*, 2001, 42: 860-867.

71. Choi HB, Ryu JK, Kim SU, McLarnon JG. Modulation of the purinergic P2X7 receptor attenuates lipopolysaccharide-mediated microglial activation and neuronal damage in inflamed brain. *J Neurosci*, 2007, 27: 4957-4968.

72. McLarnon JG, Ryu JK, Walker DG, Choi HB. Upregulated expression of purinergic P2X7 receptor in Alzheimer disease and amyloid-β peptide-treated microglia and in peptide-injected rat hippocampus. *J Neuropathol Exp Neurol*, 2006, 65: 1090-1097.

73. Sanz JM, Chiozzi P, Ferrari D, Colaianna M, Idzko M, Falzoni S, Fellin R, Trabace L, Di Virgilio F. Activation of microglia by amyloid {beta} requires P2X7 receptor expression. *J Immunol*, 2009, 182(7): 4378-4385.

74. Vianna EP, Ferreira AT, Naffah-Mazzacoratti MG, Sanabria ER, Funke M, Cavalheiro EA, Fernandes MJ. Evidence that ATP participates in the pathophysiology of pilocarpine-induced temporal lobe epilepsy: fluorimetric, immunohistochemical, and Western blot studies. *Epilepsia*, 2002, 5: 227–229.

75. Franke H., Günther A, Grosche J, Schmidt R, Rossner S, Reinhardt R, Faber-Zuschratter H, Schneider D, Illes P. P2X7 receptor expression after ischemia in the cerebral cortex of rats. *J Neuropathol Exp Neurol*, 2004, 63(7): 686-699.

76. Yanagisawa D, Kitamura Y, Takata K, Hide I, Nakata Y, Taniguchi T. Possible involvement of P2X7 receptor activation in microglial neuroprotection against focal cerebral ischemia in rats. *Biol Pharm Bull*, 2008, 31: 1121-1130.

77. Le Feuvre RA, Broug D, Touzani O, Rothwell NJ. Role of P2X7 receptors in ischemic and excitotoxic brain injury in vivo. *J Cereb Blood Flow Metab*, 2003, 23: 381-384.

78. Yiangou Y, Facer P, Durrenberger P, Chessel IP, Naylor A, Bountra C, Banat RR, Anand P. COX-2, CB2 and P2X7-immunoreactivities are increased in activated microglial cells/macrophages of multiple sclerosis and amyotrophic lateral sclerosis spinal cord. *BMC Neurol*, 2006, 6: 12.

79. D'Ambrosi, Finocchi P, Apolloni S, Cozzolino M, Ferri A, Padovano V, Pietrini G, Carrì MT, Volonté C. The proinflammatory action of microglial P2 receptors is enhanced in SOD1 models for amyotrophic lateral sclerosis. *J Immunol*, 2009, 183(7): 4648-4656.

80. Gandelman M, Peluffo H, Beckman JS, Cassina P, Barbeito L. Extracellular ATP and the P2X7 receptor in astrocyte-mediated motor neuron death: implications for amyotrophic lateral sclerosis. *J Neuroinflammation*, 2010, 7: 33.

81. Warren S, Warren KG. Prevalence of multiple sclerosis in Barrhead County, Alberta, Canada. Can. *J Neurol Sci*, 1992, 19: 72–75.

82. Wynn DR, Rodriguez M, O'Fallon WM, Kurland LT. A reappraisal of the epidemiology of multiple sclerosis in Olmsted County, Minnesota. *Neurology*, 1990, 40: 780–786.

83. Simpson S, Blizzard L, Otahal P, van der Mei I, Taylor B. Latitude is significantly associated with the prevalence of multiple sclerosis: A meta-analysis. *J Neurol Neurosurg Psychiatry*, 2011, 82: 1132–1141.

84. Compston A. Genetic epidemiology of multiple sclerosis. *J Neurol Neurosurg Psychiatry*, 1997, 62: 553–561.

85. Beebe GW, Kurtzke JF, Kurland LT, Auth TL, Nagler B. Studies on the natural history of multiple sclerosis. 3. Epidemiologic analysis of the army experience in World War II. *Neurology*,1967, 17: 1–17.

86. Kurtzke JF. A reassessment of the distribution of multiple sclerosis. Part one. *Acta Neurol Scand*, 1975, 51: 110–136.

87. Visser EM, Wilde K, Wilson JF, Yong KK, Counsell CE. A new prevalence study of multiple sclerosis in Orkney, Shetland and Aberdeen city. *J Neurol Neurosurg Psychiatry*, 2012, 83: 719–724.

88. Brain W. Diseases of the Nervous System. 3rd ed. Oxford Medical Publications; London, UK: p. 1947.

89. Barnett MH, Williams DB, Day S, Macaskill P, McLeod JG. Progressive increase in incidence and prevalence of multiple sclerosis in Newcastle, Australia: A 35-year study. *J Neurol Sci*, 2003, 213: 1-6.

90. Etemadifar M, Maghzi AH. Sharp increase in the incidence and prevalence of multiple sclerosis in Isfahan, Iran. *Mult Scler*, 2011, 17: 1022-1027.

91. Koch-Henriksen N, Sorensen PS. The changing demographic pattern of multiple sclerosis epidemiology. *Lancet Neurol*, 2010, 9: 520-532.

92. Taylor BV, Lucas RM, Dear K, Kilpatrick TJ, Pender MP, van der Mei IA, Chapman C, Coulthard A, Dwyer T, McMichael AJ, Valery PC, Williams D, Ponsonby AL. Latitudinal variation in incidence and type of first central nervous system demyelinating events. *Mult Scler*, 2010, 16: 398-405.

93. Palacios N, Alonso A, Bronnum-Hansen H, Ascherio A. Smoking and increased risk of multiple sclerosis: Parallel trends in the sex ratio reinforce the evidence. *Ann Epidemiol*, 2011, 21: 536-542.

94. Wallin MT, Culpepper WJ, Coffman P, Pulaski S, Maloni H, Mahan CM, Haselkorn JK, Kurtzke JF. Veterans Affairs Multiple Sclerosis Centres of Excellence Epidemiology Group. The Gulf War era multiple sclerosis cohort: Age and incidence rates by race, sex and service. *Brain*, 2012, 135: 1778-1785.

95. Gale CR, Martyn CN. Migrant studies in multiple sclerosis. *Prog Neurobiol*, 1995, 47: 425-448.

96. Ahlgren C, Lycke J, Odén A, Andersen O. High risk of MS in Iranian immigrants in Gothenburg, Sweden. *Mult Scler*, 2010, 16: 1079–1082.

97. McLeod JG, Hammond SR, Kurtzke JF. Migration and multiple sclerosis in immigrants to Australia from United Kingdom and Ireland: A reassessment. I. Risk of MS by age at immigration. *J Neurol*, 2011, 258: 1140–1149.

98. Handel AE, Williamson AJ, Disanto G, Dobson R, Giovannoni G, Ramagopalan SV. Smoking and multiple sclerosis: An updated meta-analysis. *PLoS One*, 2011, 6: e16149.

99. Handel AE, Williamson AJ, Disanto G, Handunnetthi L, Giovannoni G, Ramagopalan SV. An updated meta-analysis of risk of multiple sclerosis following infectious mononucleosis. *PLoS One*, 2010, 5: e12496.

100. Islam T, Gauderman WJ, Cozen W, Mack TM. Childhood sun exposure influences risk of multiple sclerosis in monozygotic twins. *Neurology*, 2007, 69: 381–388.

101. Van der Mei IA, Ponsonby AL, Dwyer T, Blizzard L, Simmons R, Taylor BV, Butzkueven H, Kilpatrick T. Past exposure to sun, skin phenotype, and risk of multiple sclerosis: Case-control study. *Br Med J*, 2003, 327: 316.

102. O'Gorman C, Lucas R, Taylor B. Environmental risk factors for multiple sclerosis: a review with a focus on molecular mechanisms. *Int J Mol Sci*, 2012, 13(9): 11718-52.

103. Jersild C, Svejgaard A, Fog T. HL-A antigens and multiple sclerosis. *Lancet*, 1972, 1: 1240–1241.

104. Hauser SL, Goodin DS. Multiple sclerosis and other demyelinating diseases. In: Longo DI ed. Harrison's Principles of Internal Medicine, 18th edn. New York: McGraw-Hill, 2012: 3395–3409.

105. Naito S, Namerow N, Mickey MR, Terasaki PI. Multiple sclerosis: association with HL-A3. *Tissue Antigens*, 1972, 2: 1–4.

106. Olerup O, Hillert J. HLA class II-associated genetic susceptibility in multiple sclerosis: a critical evaluation. *Tissue Antigens*, 1991, 38: 1–15.

107. Barcellos LF, et al. Heterogeneity at the HLA-DRB1 locus and risk for multiple sclerosis. *Hum Mol Genet*, 2006, 15: 2813–2824.

108. Sawcer S, et al. Genetic risk and a primary role for cell-mediated immune mechanisms in multiple sclerosis. *Nature*, 2011, 476: 214–219.

109. Gourraud PA, Harbo HF, Hauser SL, Baranzini SE. The genetics of multiple sclerosis: an up-to-date review. *Immunol Rev*, 2012, 248(1): 87-103.

110. Rovaris M, Confavreux C, Furlan R, Kappos L, Comi G, Filippi M. Secondary progressive multiple sclerosis: current knowledge and future challenges. *Lancet Neurol*, 2006, 5: 343–354.

111. Stadelmann C, Albert M, Wegner C, Bruck W. Cortical pathology in multiple sclerosis. *Curr Opin Neurol*, 2008, 21: 229–234.

112. Lassmann H. (2007) Cortical, subcortical and spinal alterations in neuroimmunological diseases. *J Neurol*, 2007, 254: 15–17.

113. He F, Sun YE. Glial cells more than support cells? *Int J Biochem Cell Biol*, 2007, 39: 661–666.

114. Williams A, Piaton G, Lubetzki C. Astrocytes–friends or foes in multiple sclerosis? *Glia*, 2007, 55: 1300–1312.

115. Muzio L, Martino G, Furlan R. Multifaceted aspects of inflammation in multiple sclerosis: the role of microglia. *J Neuroimmunol*, 2007, 191: 39–44.

116. Sanders P, De Keyser J. Janus faces of microglia in multiple sclerosis. *Brain Res Rev*, 2007, 54: 274-285.

117. Amadio S, Apolloni S, D'Ambrosi N, Volonté C. Purinergic signalling at the plasma membrane: a multipurpose and multidirectional mode to deal with amyotrophic lateral sclerosis and multiple sclerosis. *J Neurochem*, 2011, 116(5): 796-805.

118. Agresti C, Meomartini ME, Amadio S, Ambrosini E, Serafini B, Franchini L, Volonte´ C, Aloisi F, Visentin S. Metabotropic P2 receptor activation regulates oligodendrocyte progenitor migration and development. *Glia*,2005, 50: 132–144.

119. Frischer JM, Bramow S, Dal-Bianco A, Lucchinetti CF, Rauschka H, Schmidbauer M, Laursen H, Sorensen PS, Lassmann H. The relation between inflammation and neurodegeneration in multiple sclerosis. *Brain*, 2009, 132: 1175–1189.

120. Prineas JW, Wright RG. Macrophages, lymphocytes, and plasma cells in the perivascular compartment in chronic multiple sclerosis. *Lab. Invest,* 1978, 38: 409–421.

121. Babbe H, Roers A, Waisman A, Lassmann H, Goebels N, Hohlfeld R, Friese M, Schröder R, Deckert M, Schmidt S, Ravid R, Rajewsky K. Clonal expansion of $CD8^+$ T cells dominate the T cell infiltrate in active multiple sclerosis lesions as shown by micromanipulation and single cell polymerase chain reaction. *J Exp Med, 2000,* 192: 393–404.

122. Barnett MH, Prineas JW. Relapsing and remitting multiple sclerosis: pathology of the newly forming lesion. *Ann Neurol,* 2004, 55: 458–468.

123. Marik C, Felts P, Bauer J, Lassmann H, Smith KJ. Lesion genesis in a subset of patients with multiple sclerosis: a role for innate immunity? *Brain*, 2007, 130: 2800–2815.

124. Henderson AP, Barnett MH, Parratt JD, Prineas JW. Multiple sclerosis: distribution of inflammatory cells in newly forming lesions. *Ann Neurol,* 2009, 66: 739–753.

125. Grossman RI, Braffman BH, Brorson JR, Goldberg HI, Silberberg DH, Gonzalez-Scarano F. Multiple sclerosis: serial study of gadolinium enhanced MR imaging. *Radiology, 1988*, 169: 117–122.

126. Gaitán MI, Shea CD, Evangelou IE, Stone RD, Fenton KM, Bielekova B, Massacesi L, Reich DS. Evolution of the blood brain barrier in newly forming multiple sclerosis lesions. *Ann Neurol, 2011,* 70: 22–29.

127. Hochmeister S, Grundtner R, Bauer J, Engelhardt B, Lyck R, Gordon G, Korosec T, Kutzelnigg A, Berger JJ, Bradl M, Bittner RE, Lassmann H. Dysferlin is a new marker for leaky brain blood vessels in multiple sclerosis. *J Neuropathol Exp Neurol, 2006,* 65: 855–865.

128. Kwon EE, Prineas JW. Blood–brain barrier abnormalities in longstanding multiple sclerosis lesions. An immunohistochemical study. *J Neuropathol Exp Neurol,* 1994, 53: 625–636.

129. Kirk J, Plumb J, Mirakhur M, McQuaid S. Tight junctional abnormality in multiple sclerosis white matter affects all calibres of vessel and is associated with blood–brain barrier leakage and active demyelination. *J Pathol,* 2003, 201: 319–327.

130. Serafini B, Rosicarelli B, Magliozzi R, Stigliano E, Aloisi F. Detection of ectopic B-cell follicles with germinal centers in the meninges of patients with secondary progressive multiple sclerosis. *Brain Pathol,* 2004, 14: 164–174.

131. Howell OW, Reeves CA, Nicholas R, Carassiti D, Radotra B, Gentleman SM, Serafini B, Aloisi F, Roncaroli F, Magliozzi R, Reynolds R. Meningeal inflammation is widespread and linked to cortical pathology in multiple sclerosis. *Brain,* 2011, 134: 2755–2771.

132. Lassmann H, van Horssen J, Mahad. Progressive multiple sclerosis: pathology and pathogenesis. *D Nat Rev Neurol*, 2012, 5;8(11): 647-656.

133. Allen IV, McQuaid S, Mirakhur M, et al. Pathological abnormalities in the normal-appearing white matter in multiple sclerosis. *Neurol Sci*, 2001; 22: 141.

134. Wu GF, Alvarez E. The immunopathophysiology of multiple sclerosis. *Neurol Clin*, 2011, 29(2): 257-278.

135. Kawai T, Andrews D, Colvin RB, Sachs DH, Cosimi AB. Thromboembolic complications after treatment with monoclonal antibody against CD40 ligand. *Nat Med*, 2000, 6(2): 114

136. Fromont A, De Seze J, Fleury MC, Maillefert JF, Moreau T. Inflammatory demyelinating events following treatment with anti-tumor necrosis factor. *Cytokine*, 2009, 45(2): 55–57

137. Storch MK, Bauer J, Linington C, Olsson T, Weissert R, Lassmann H. Cortical demyelination can be modeled in specific rat models of autoimmune encephalomyelitis and is major histocompatability complex (MHC) haplotype-related. *J Neuropathol Exp Neurol*, 2006, 65: 1137–1142

138. Weissert R, Wallström E, Storch MK, Stefferl A, Lorentzen J, Lassmann H, Linington C, Olsson T. MHC haplotype-dependent regulation of MOG-induced EAE in rats. *J Clin Invest*, 1998, 102: 1265–1273.

139. 't Hart BA, Gran B, Weissert R. EAE: imperfect but useful models of multiple sclerosis. *Trends Mol Med*, 2011, 17(3): 119-125.

140. Dong M, Liu R, Guo L, Li C, Tan G. Pathological findings in rats with experimental allergic encephalomyelitis. *APMIS*, 2008, 116(11): 972-984.

141. Inoue K, Koizumi S, Tsuda M. The role of nucleotides in the neuron–glia communication responsible for the brain functions. *J Neurochem*, 2007, 102: 1447–1458.

142. Apolloni S, Montilli C, Finocchi P, Amadio S. Membrane compartments and purinergic signaling: P2X receptors in neurodegenerative and neuroinflammatory events. *FEBS J*, 2009, 276: 354–364.

143. Stevens B, Porta S, Haak LL, Gallo V, Fields RD. Adenosine: a neuron–glial transmitter promoting myelination in the CNS in response to action potentials. *Neuron*, 2002, 36:855–868.

144. Othman T, Yan H, Rivkees SA. Oligodendrocytes express functional A1 adenosine receptors that stimulate cellular migration. *Glia*, 2003, 44: 166–172.

145. Mora´n-Jime´nez MJ, Matute C. Immunohistochemical localization of the P2Y(1) purinergic receptor in neurons and glial cells of the central nervous system. *Brain Res Mol Brain Res*, 2000, 78: 50–58.

146. James G, Butt AM. P2X and P2Y purinoreceptors mediate ATP-evoked calcium signalling in optic nerve glia in situ. *Cell Calcium*, 2001, 30: 251–259.

147. Agresti C, Meomartini ME, Amadio S, Ambrosini E, Serafini B, Franchini L, Volonte´ C, Aloisi F, Visentin S. Metabotropic P2 receptor activation regulates oligodendrocyte progenitor migration and development. *Glia*, 2005, 50: 132–144.

148. Alberdi E, Sanchez-Gomez MV, Marino A, Matute C. Ca(21) influx through AMPA or kainate receptors alone is sufficient to initiate excitotoxicity in cultured oligodendrocytes. *Neurobiol Dis*, 2002, 9: 234–243.

149. Butt AM, Hamilton N, Hubbard P, Pugh M, Ibrahim M. Synantocytes: The fifth element. *J Anat*, 2005, 207: 695–706.

150. Ishibashi T, Dakin K, Stevens B, Lee P, Kozlov S, Stewart C, Fields R. Astrocytes promote myelination in response to electrical impulses. *Neuron* 2006, 49: 823–832.

151. Guo LH, Schluesener HJ. Lesional accumulation of P2X4 receptor+ macrophages in rat CNS during experimental autoimmune encephalomyelitis. *Neuroscience*,2005, 34: 99–205.

152. Amadio S, Montilli C, Magliozzi R, Bernardi G, Reynolds R, Volonte´ C. P2Y12 receptor protein in cortical gray matter lesions in multiple sclerosis. *Cereb Cortex*, 2010, 20: 1263–1273.

153. Yiangou Y, Facer P, Durrenberger P, Chessell IP, Naylor A, Bountra C, Banati RR, Anand P. COX-2, CB2 and P2X7-immunoreactivities are increased in activated microglial cells/ macrophages of multiple sclerosis and amyotrophic lateral sclerosis spinal cord. *BMC Neurol*, 2006, 2: 6–12.

154. Matute C, Torre I, Pe´rez-Cerda` F, Pe´rez-Samartı`n A, Alberdi E, Etxebarria E, Arranz AM, Rodrı`guez-Antigu¨edad A, Sa`nchez- Go`mez MV, Domercq M. P2X7 receptor blockade prevents ATP excitotoxicity in oligodendrocytes and ameliorates experimental autoimmune encephalomyelitis. *J Neurosci*, 2007, 7: 9525–9533.

155. Sharp AJ, Polak PE, Simonini V, Lin SX, Richardson JC, Bongarzone ER, Feinstein DL. P2X7 deficiency suppresses development of experimental autoimmune ancephalomyelitis. *J Neuroinflam*, 2008, 5: 33.

156. Chen L, Brosnan CF. Exacerbation of experimental autoimmune encephalomyelitis in P2X7R-/- mice: evidence for loss of apoptotic activity in lymphocytes. *J Immunol*, 2006, 176: 3115–3126.

157. Caragnano M, Tortorella P, Bergami A, Ruggieri M, Livrea P, Specchio LM, Martino G, Trojano M, Furlan R, Avolio C. Monocytes P2X7 purinergic receptor is modulated by glatiramer acetate in multiple sclerosis. *J Neuroimmunol*, 2012, 245(1-2): 93-97.

158. Aloe L, Micera A. A role of nerve growth factor in oligodendrocyte growth and differentiation of EAE affected rats. *Arch Ital Biol*, 1998, 136(4): 247-56.

159. Willenborg DO, Staten EA, Witting GF. Experimental allergic encephalomyelitis: modulation by intraventricular injection of myelin basic protein. *Exp Neurol*, 1978, 61(3): 527-36.

160. Porsolt RD, Le Pichon M, Jalfre M. Depression: a new animal model sensitive to antidepressant treatments. *Nature*, 1977, 266(5604): 730-2.

161. Beeton C, Garcia A, Chandy KG. Induction and clinical scoring of chronic-relapsing experimental autoimmune encephalomyelitis. *J Vis Exp*, 2007, (5): 224.

162. Almolda B, González B, Castellano B. Activated microglial cells acquire an immature dendritic cell phenotype and may terminate the immune response in an acute model of EAE. *J Neuroimmunol*, 2010, 223(1-2): 39-54.

163. Constantinescu CS, Farooqi N, O'Brien K, Gran B. Experimental autoimmune encephalomyelitis (EAE) as a model for multiple sclerosis (MS). *Br J Pharmacol*,2011, 164(4): 1079-1106.

164. McFarland HF, Martin R. Multiple sclerosis: a complicated picture of autoimmunity. *Nat Immunol*, 2007, 9: 913–919.

165. Williams A, Piaton G, Lubetzki C. Astrocytes--friends or foes in multiple sclerosis? *Glia*, 2007; 55:1300–1312.

166. Matsumoto Y, Ohmori K, Fujiwara M. Microglial and astroglial reactions to inflammatory lesions of experimental autoimmune encephalomyelitis in the rat central nervous system. *J Neuroimmunol*, 1992, 37(1-2): 23-33.

167. Brown DA, Sawchenko PE: Time course and distribution of inflammatory and neurodegenerative events suggest structural bases for the pathogenesis of experimental autoimmune encephalomyelitis. *J Comp Neurol*, 2007, 502: 236-2607

168. Ajami B, Bennett JL, Krieger C, McNagny KM, Rossi FM. Infiltrating monocytes trigger EAE progression, but do not contribute to the resident microglia pool. *Nat Neurosci*, 2011, 14(9): 1142-9.

169. Wiley JS, Sluyter R, Gu BJ, Stokes L, Fuller SJ. The human P2X7 receptor and its role in innate immunity. *Tissue Antigens*, 2011, 78(5): 321-32.

170. Baricordi OR, Melchiorri L, Adinolfi E, Falzoni S, Chiozzi P, Buell G, Di Virgilio F. Increased proliferation rate of lymphoid cells transfected with the P2X(7) ATP receptor. *J Biol Chem*, 1999, 274(47): 33206-8.

171. Narcisse L, Scemes E, Zhao Y, Lee SC, Brosnan CF. The cytokine IL-1beta transiently enhances P2X7 receptor expression and function in human astrocytes. *Glia*, 2005, 49(2): 245-58.

172. Schneider C, Schuetz G, Zollner TM. Acute neuroinflammation in Lewis rats - a model for acute multiple sclerosis relapses. *J Neuroimmunol*, 2009, 213(1-2): 84-90.

173. Rossol M, Heine H, Meusch U, Quandt D, Klein C, Sweet MJ, Hauschildt S. LPS-induced cytokine production in human monocytes and macrophages. *Crit Rev Immunol*, 2011, 31(5): 379-446.

Acknowledgments

I would like to thank Prof. Franco Laghi Pasini for hosting me in his laboratory and allowing me to perform this thesis, for helping me during the PhD course and for his critical advises on the experimental work and writing of this thesis.

Thanks also to his team, Prof. Pier Leopoldo Capecchi and Dott. Pietro Enea Lazzerini for supporting me during these years.

Thanks also to Dott.ssa Cinzia Volonté for hosting me in her laboratory c/o S. Lucia Foundation in Rome during the last year of my PhD and for all the help provided.

Thanks to Prof. Luca Battistini and Dott.ssa Eleonora Piras c/o S. Lucia foundation, for advises and support with FACS experiments.

I express my gratitude to Dott.ssa Paola Tirassa c/o CNR of Rome, for teaching me the model of EAE animals and help me with these experiments.

Thanks also Prof. Richard Reynolds and the UK MS Tissue Bank for providing all post-mortem MS brain samples.

I express my deep and sincere gratitude to all my co-workers both in Siena and in Rome and, in particular, Dott.ssa Stefania Zimbone, Dott.ssa Elena Gianchecchi, Dott.ssa Monica Castrichini, Dott.ssa Maria Rita Natale, Dott.ssa Susanna Amadio, Dott.ssa Nadia D'Ambrosi, Dott.ssa Savina Apolloni and Dott.ssa Chiara Parisi, for providing me full support with experiments and advises.